HAWC: SOFIA's Facility Far-IR Camera and Polarimeter

C. Darren Dowell (Jet Propulsion Laboratory)
for the HAWC+ Collaboration

2014 August 6

Outline

- HAWC+ upgrade program and team
- elements of HAWC
- project schedule
- initial astrophysics programs

HAWC: High-resolution Airborne Wideband Camera, built by U. Chicago, P.I. Al Harper

HAWC+: upgrade program, 2013-2016, led by JPL

The completed instrument will fly as “HAWC”.

SOFIA 1G/2G Instrument Suite

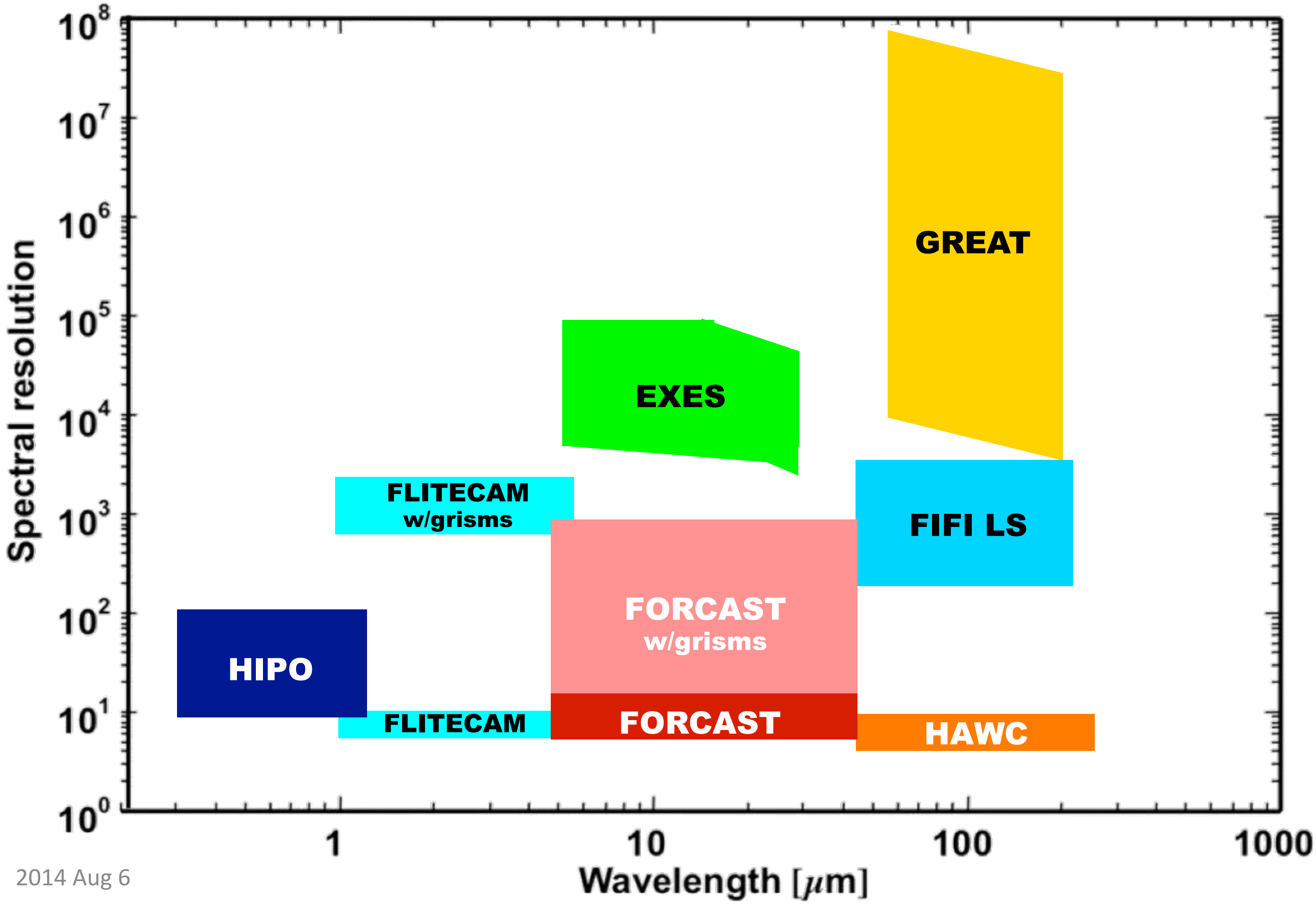

Far-IR Polarimetry: Dust & Magnetic Fields

- λ = 30 – 1000 μm continuum primarily dust emission, so *far-IR polarimetry is an indispensible probe of magnetic fields in neutral ISM*.
  - Even molecular clouds are mostly transparent at λ ≈ 100 μm.
- Multiple bands distinguish components with different temperatures.
  - Far-IR polarization spectrum also shows effects of grain emissivities.

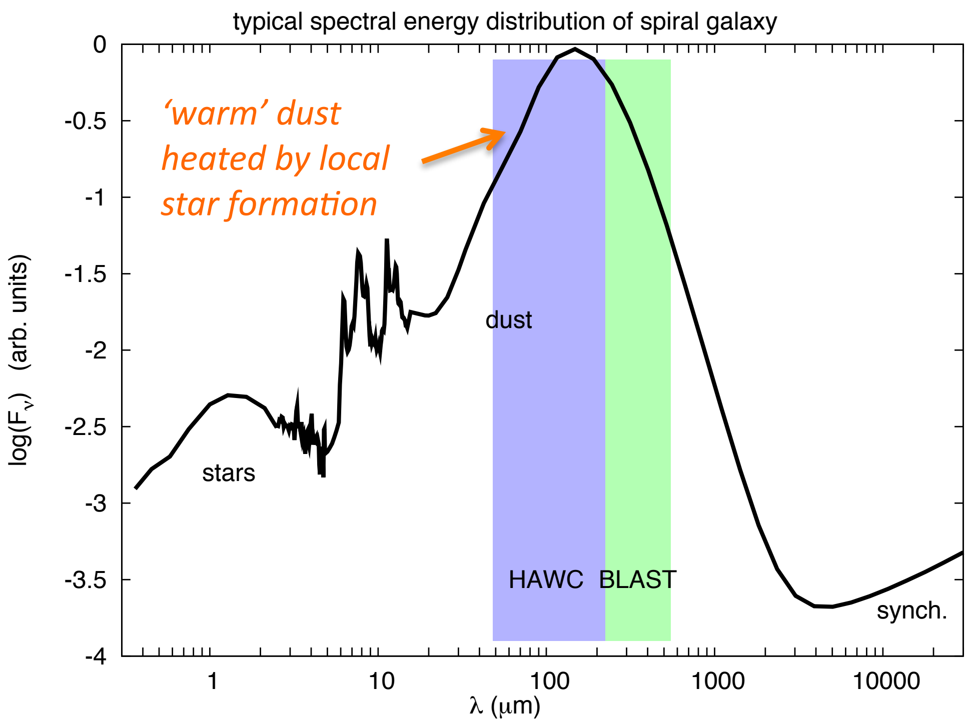

HAWC+ Upgrade Program

- April 2012: *initial selection by NASA of HAWC upgrade investigations (JPL/Dowell & Goddard/ Staguhn)*
- July 2012: *HAWC (U. Chicago) passes Pre-Ship Review*
- October 2012: *final selection and approval of merged upgrade investigation*
- February – May 2013: *co-investigators/ contractors begin funded upgrade work, toward commissioning in 2015*

HAWC+ Instrument Upgrade Team

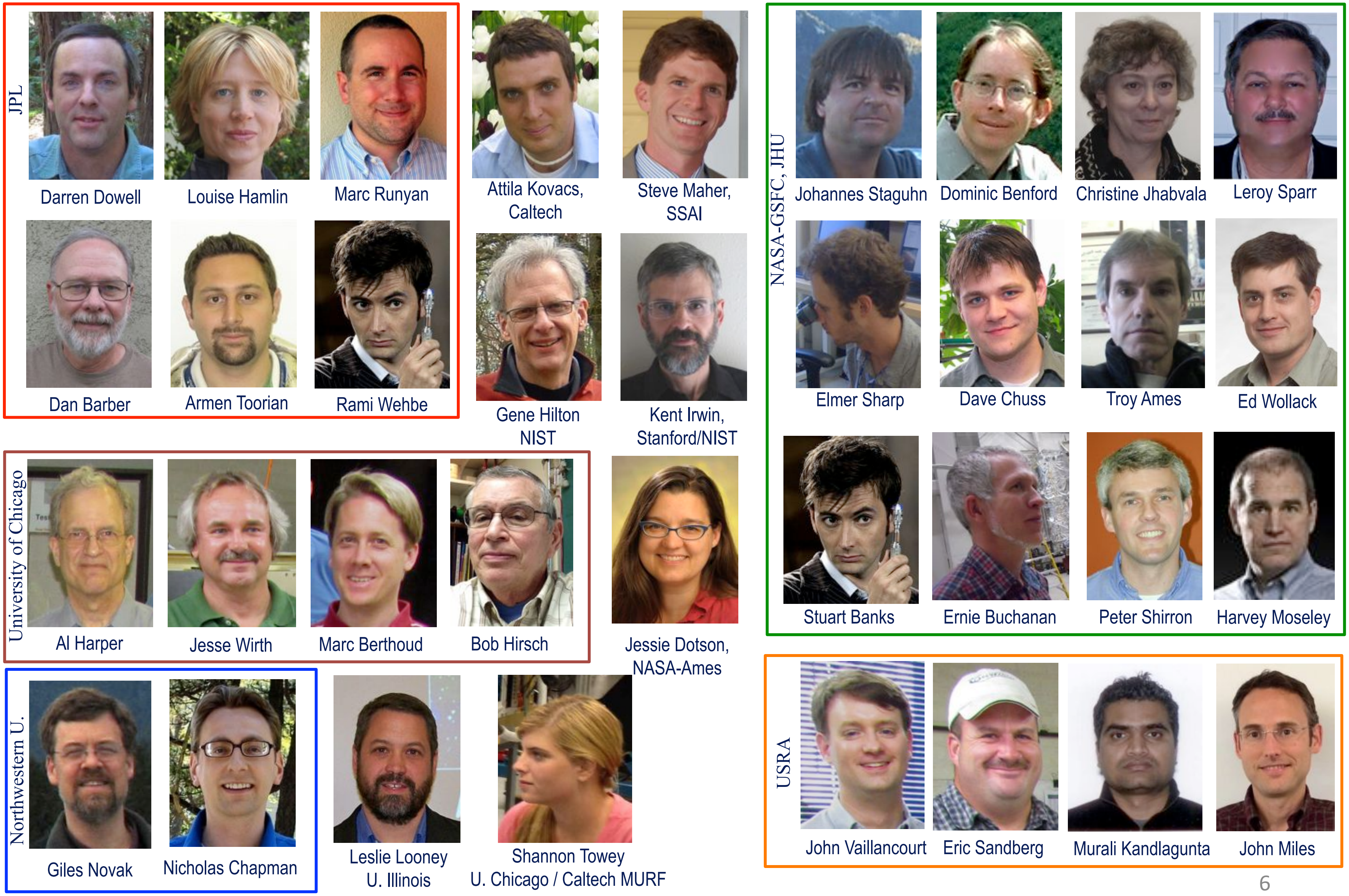

HAWC+ Builds on HAWC

HAWC at Yerkes Observatory (U. Chicago)

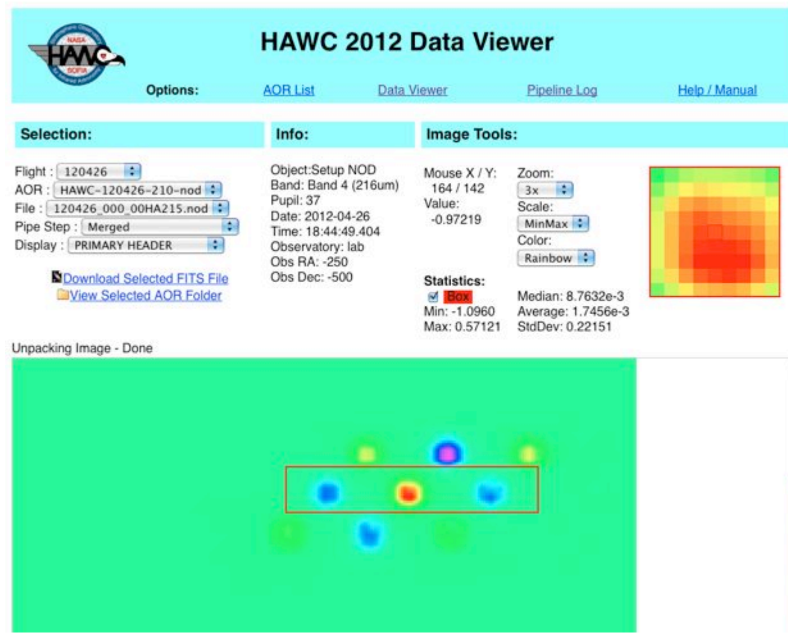

HAWC leaves Yerkes – June 3, 2013

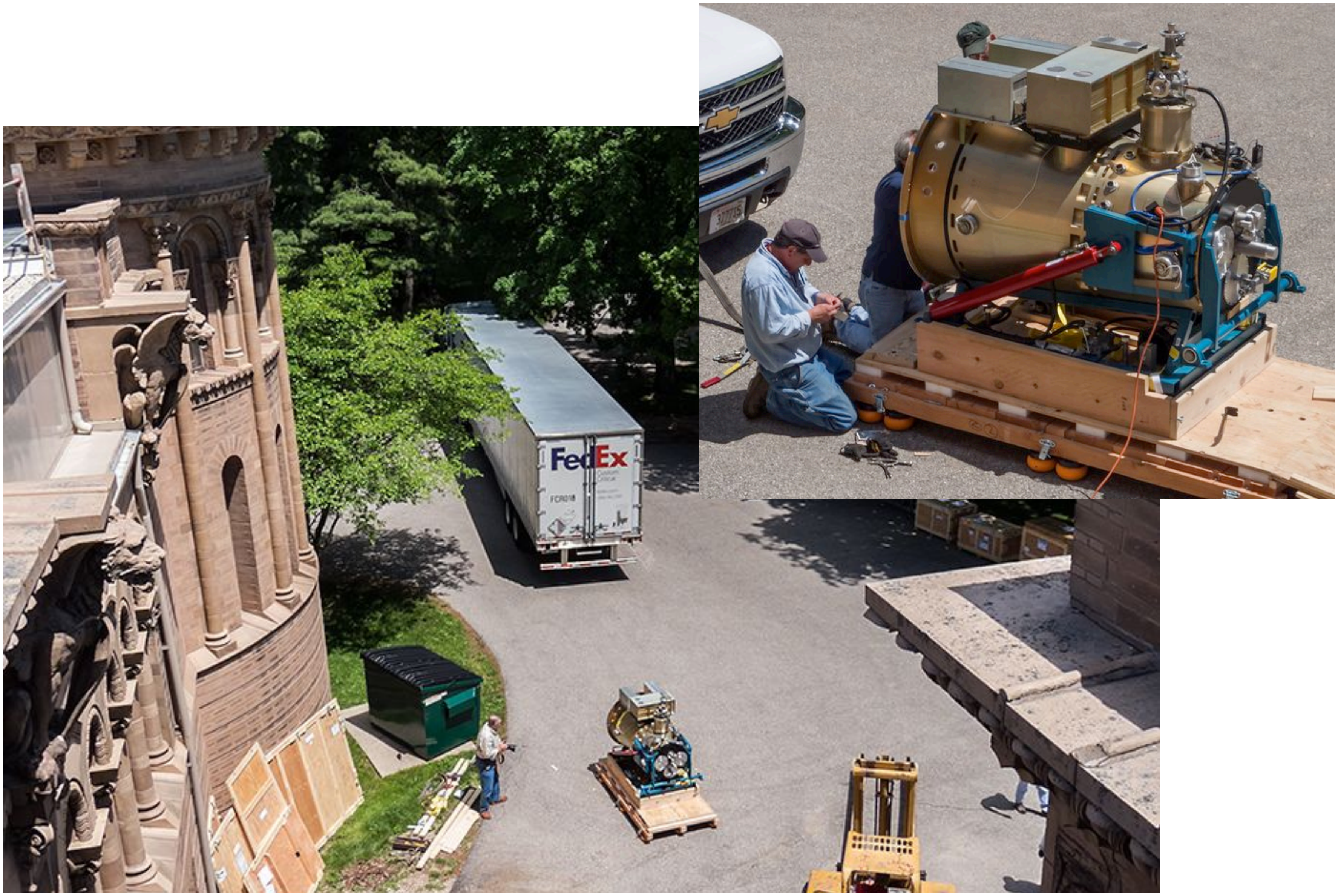

HAWC arrives at JPL – June 5, 2013

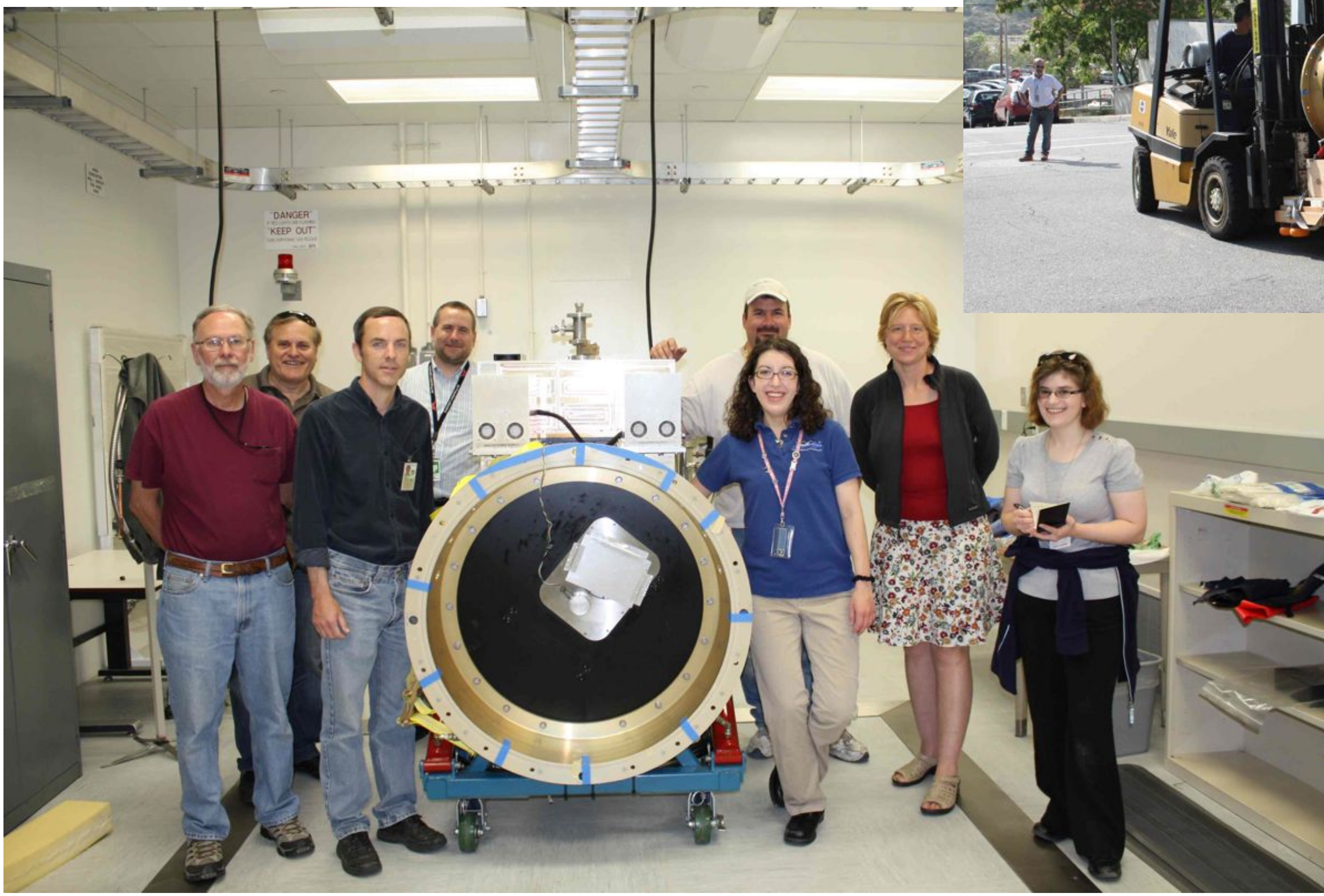

System Tests at JPL

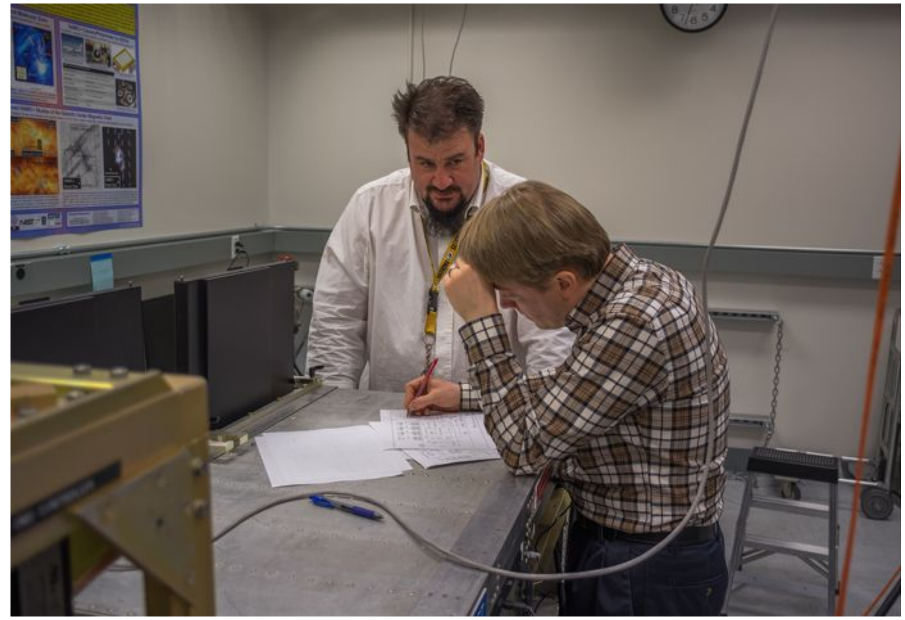

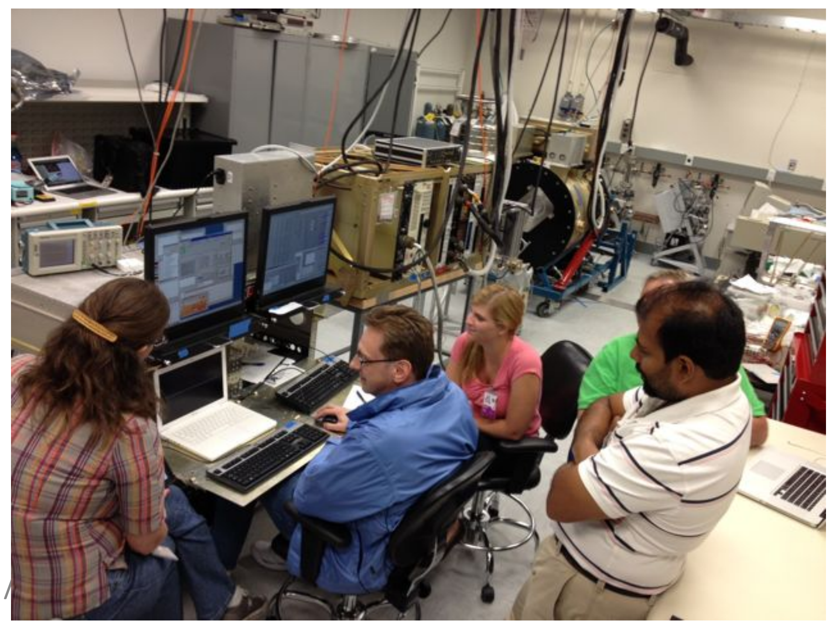

HAWC+ schematic optical path

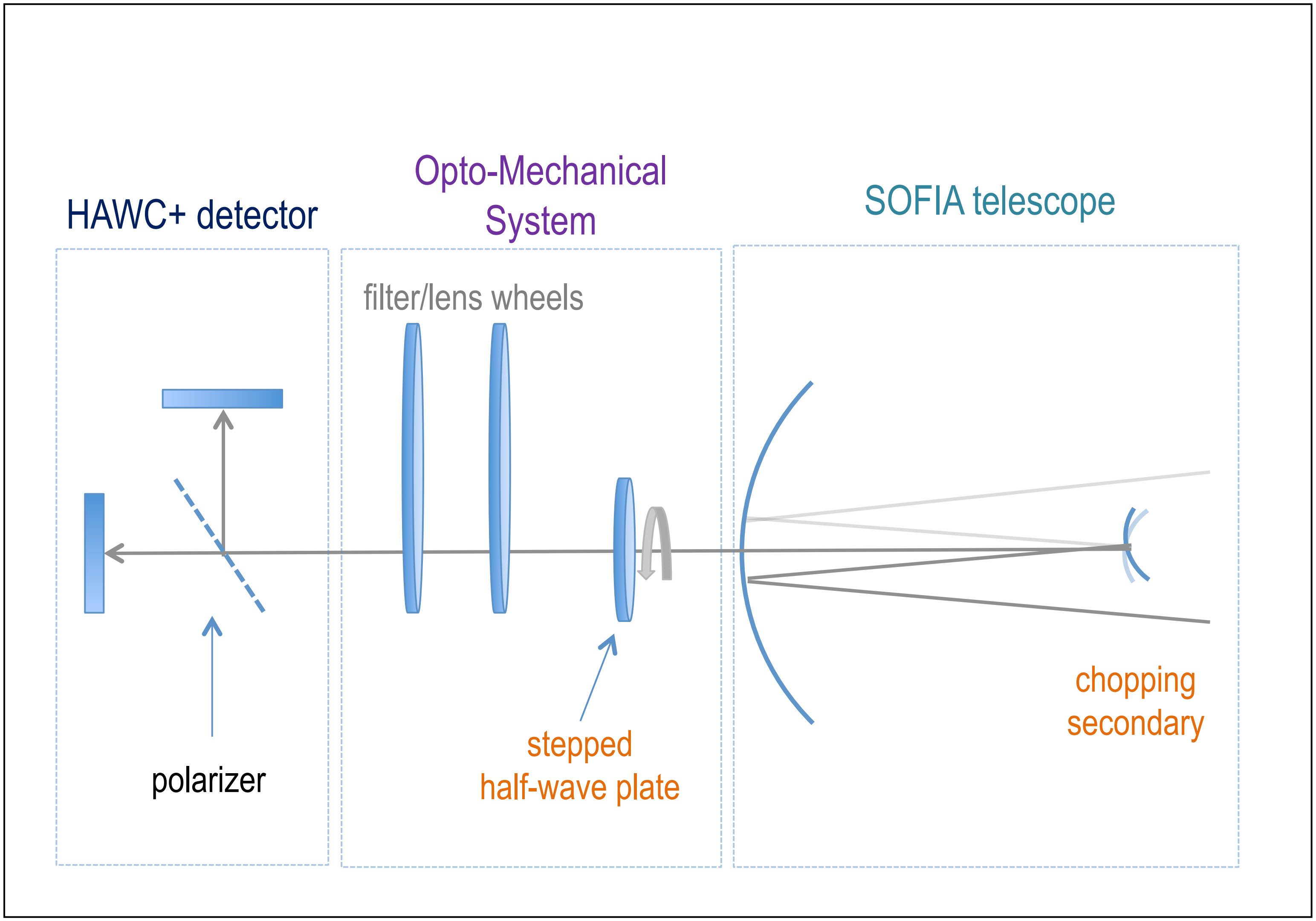

HAWC(1G) detector: 12×32

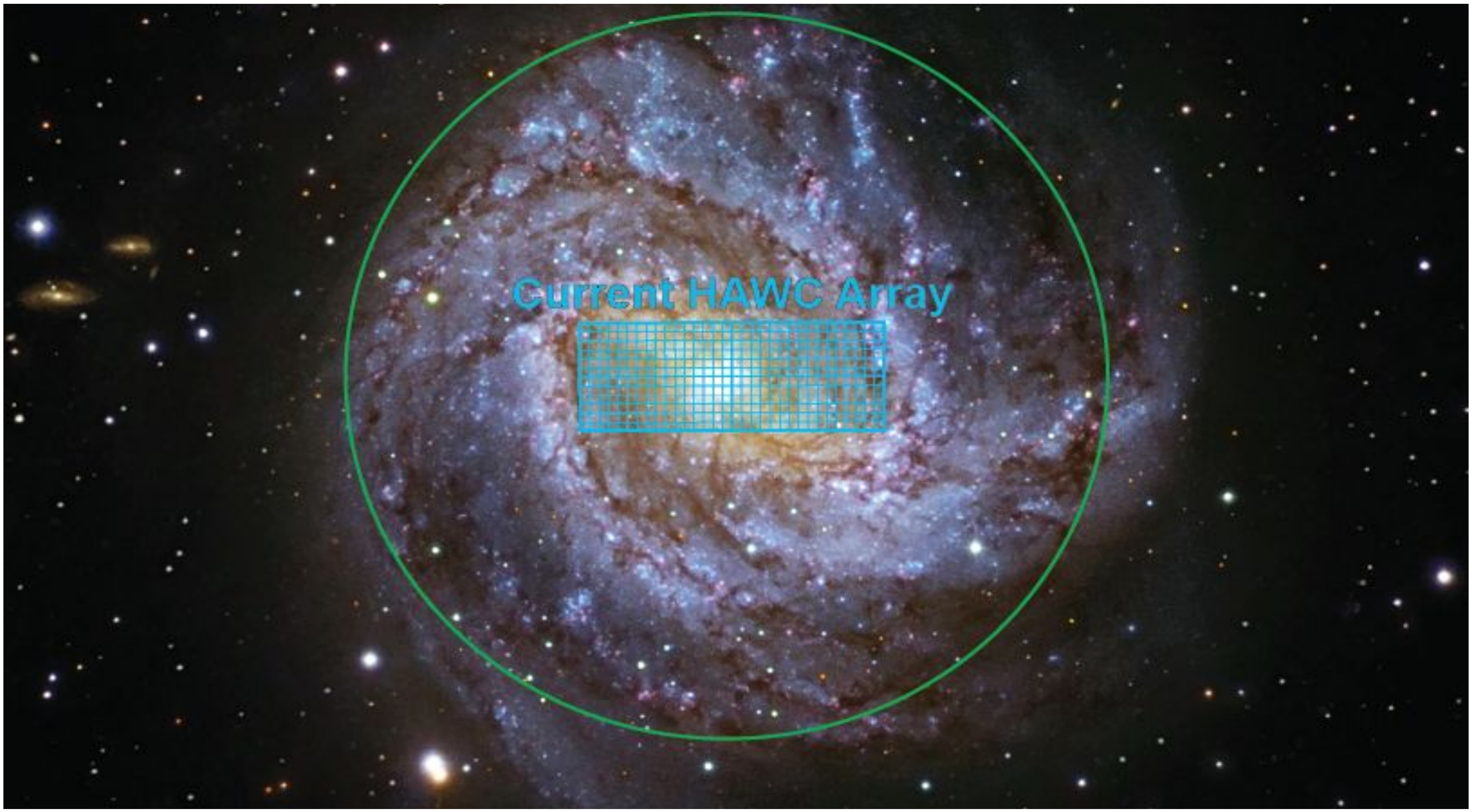

HAWC+ on SOFIA: 64×40 (design; requirement is 32×40)

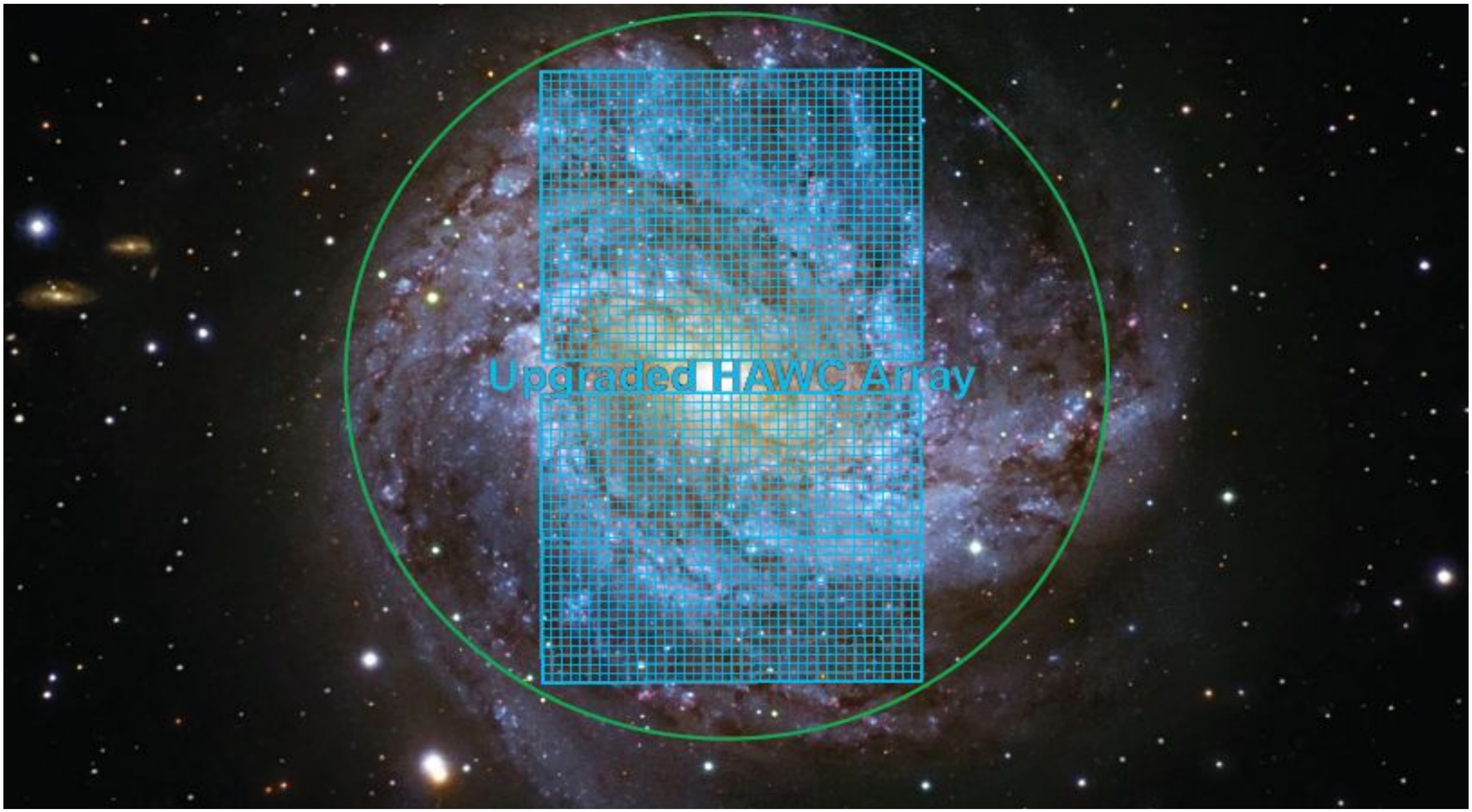

Goddard/NIST Detector Team

- Detector requirements, packaging, testing: *J. Staguhn, S. Banks, D. Benford, E. Buchanan, H. Moseley, E. Sharp, E. Wollack*
- Detector design, fab, assembly: *C. Jhabvala, T. Miller, R. Brekosky, M.-P. Chang, J. Chervenak, N. Costen, A. Datesman, E. Leong*
- SQUID Multiplexer: *G. Hilton*
- Detector subsystem management: *L. Sparr*

detector electromagnetic design: Backshort-Under-Grid architecture

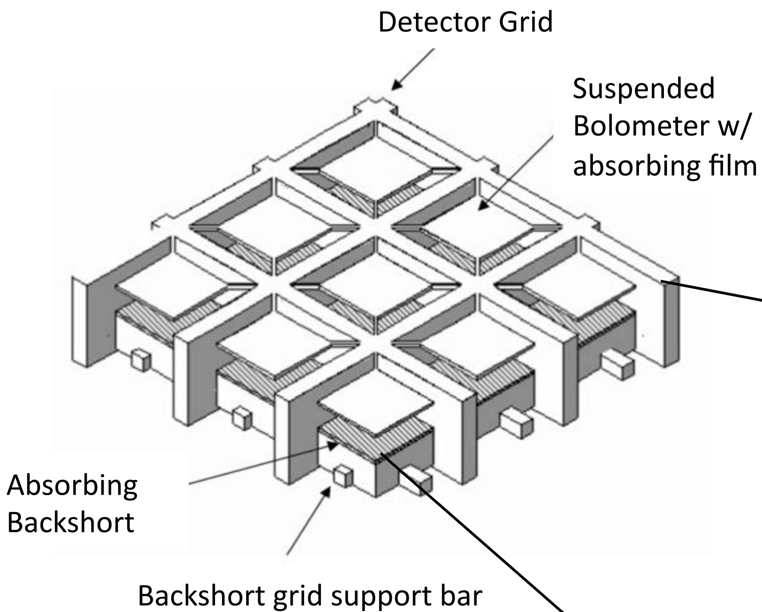

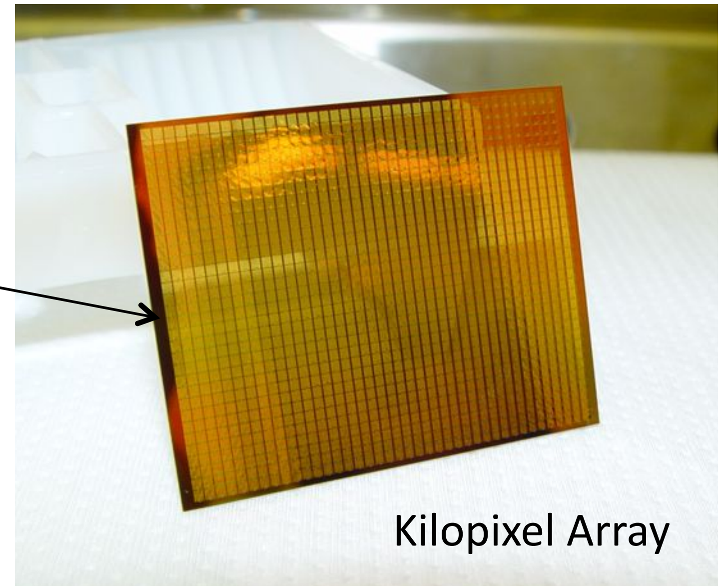

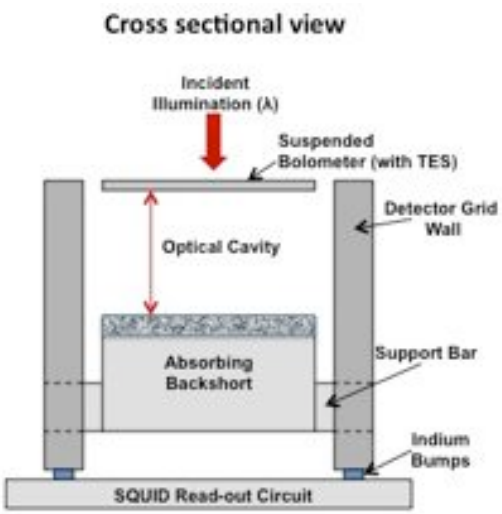

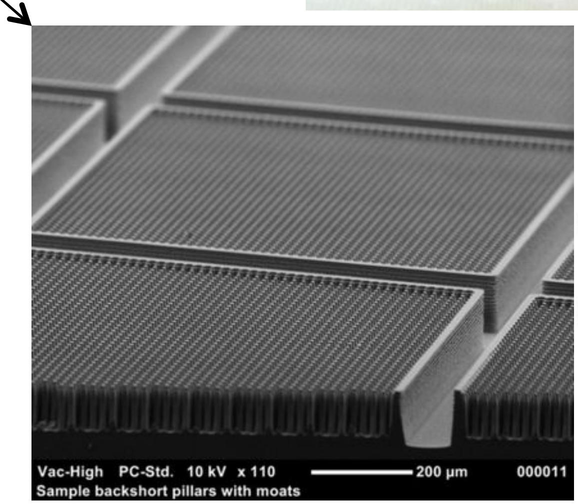

Absorbing Backshort

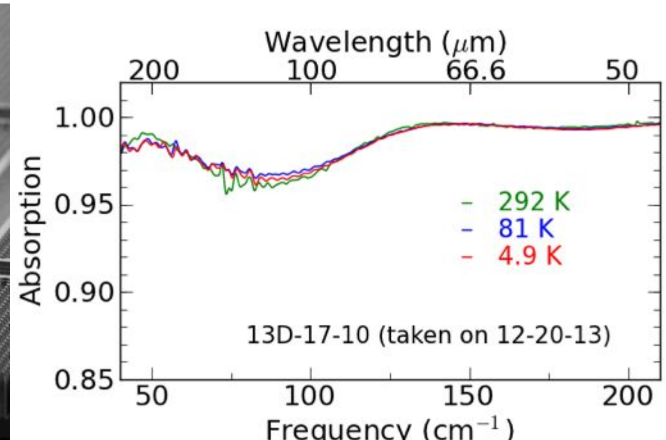

detector electrical design

- Superconducting Transition Edge Sensor (TES) bolometer

- Superconducting Quantum Interference Device (SQUID) readout

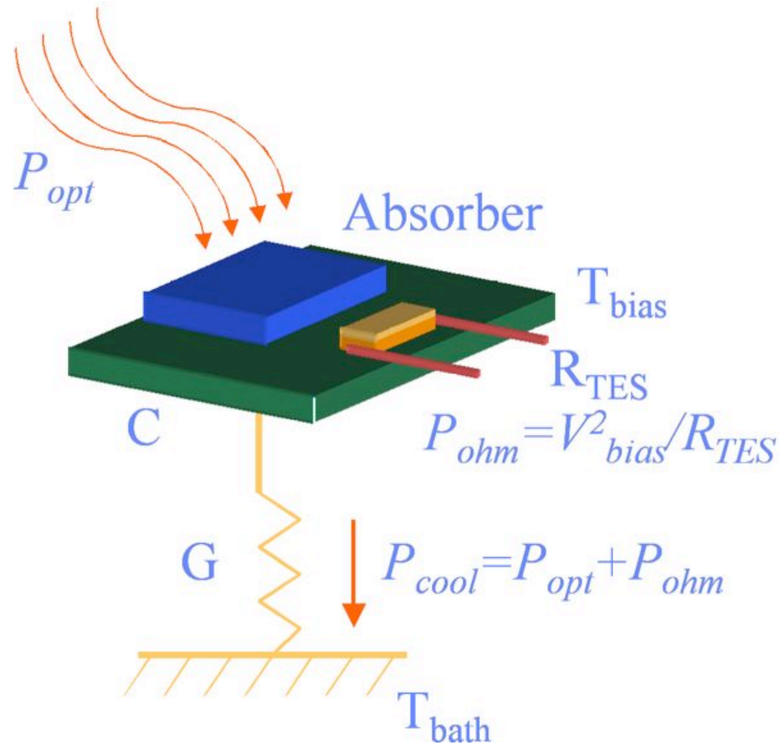

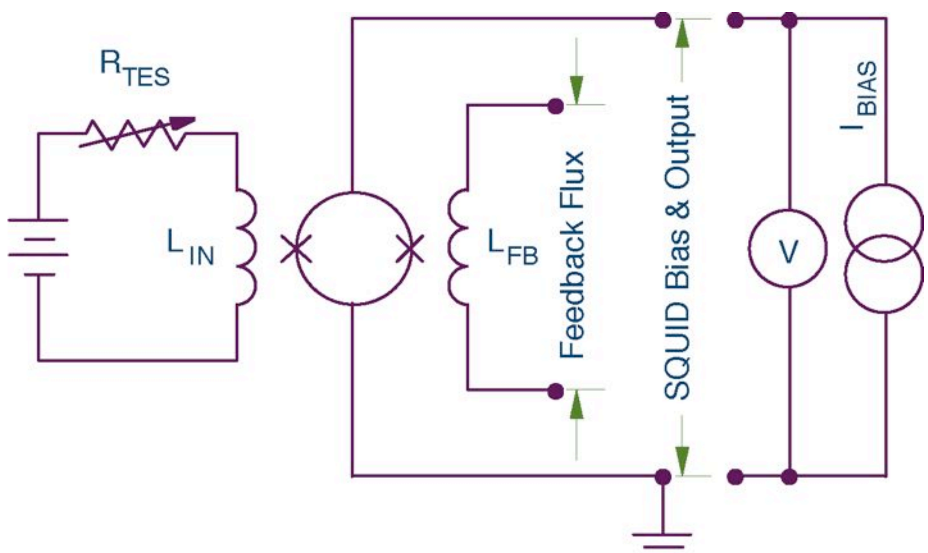

Pixel Layout

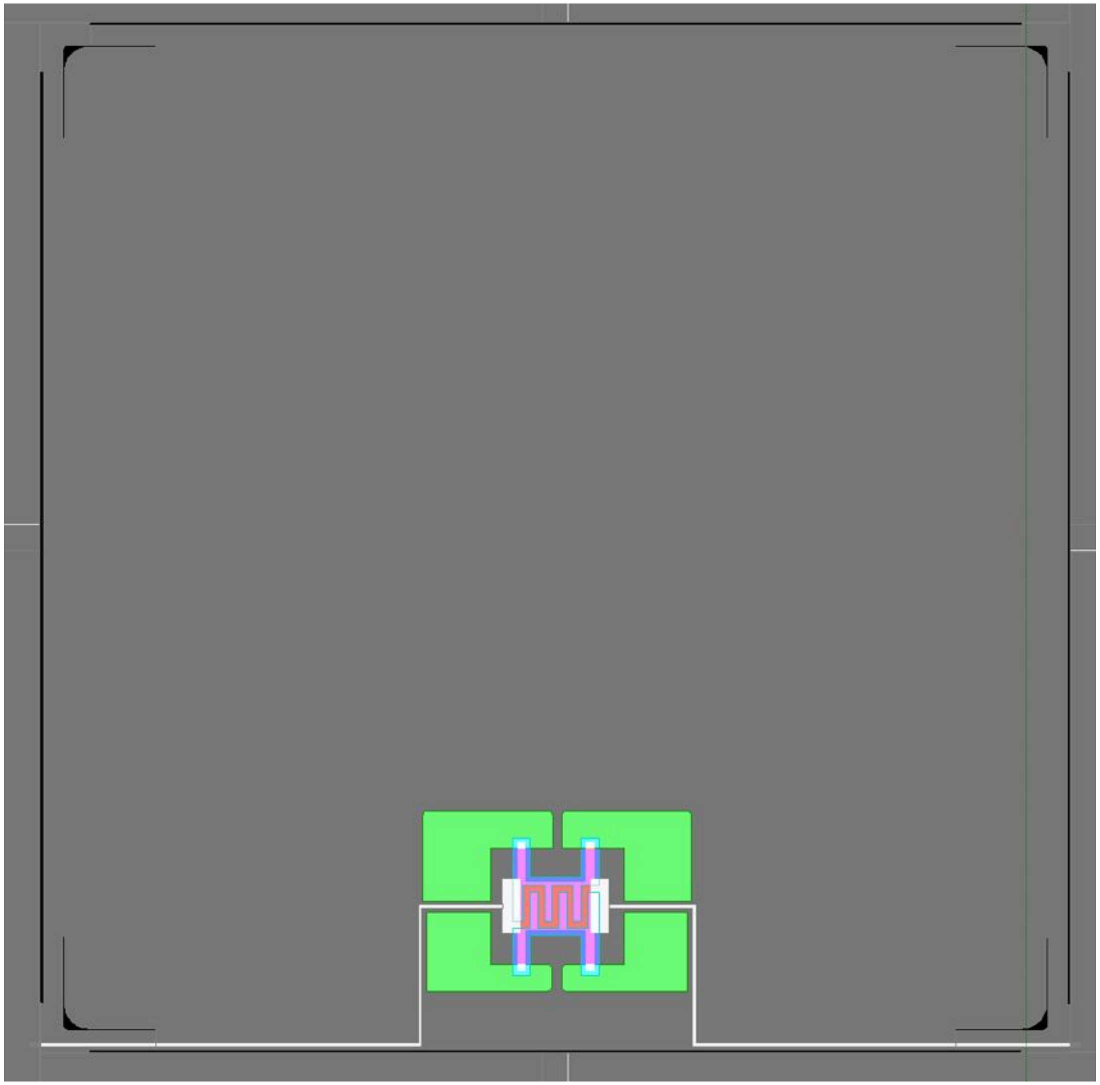

- 1.135mm pitch
- Fabricated on 1.46µm single crystal silicon

Figure Color Legend:

- Gray: Silicon membrane and frame
- White : Mo/Nb electrical leads
- Pink/Red: TES and NMBs
- Green: Palladium
- Black: Etched void (This layer etches the legs)

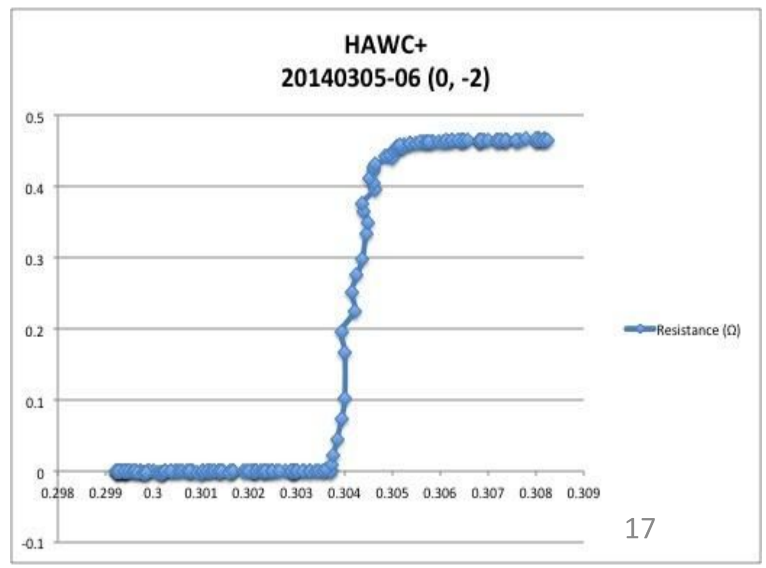

Flux-Switched Time-Domain Multiplexer

- Row Select switches current into switch inductor
- Switch critical current is large when flux is zero, hence is in superconducting state and shorts out SQUIDs → channel off
- Switch critical current near zero at some applied flux ($\Phi_0/2$) and acts like a resistor (ohms), biasing SQUIDs → channel on
- Switching set by geometry of inductance

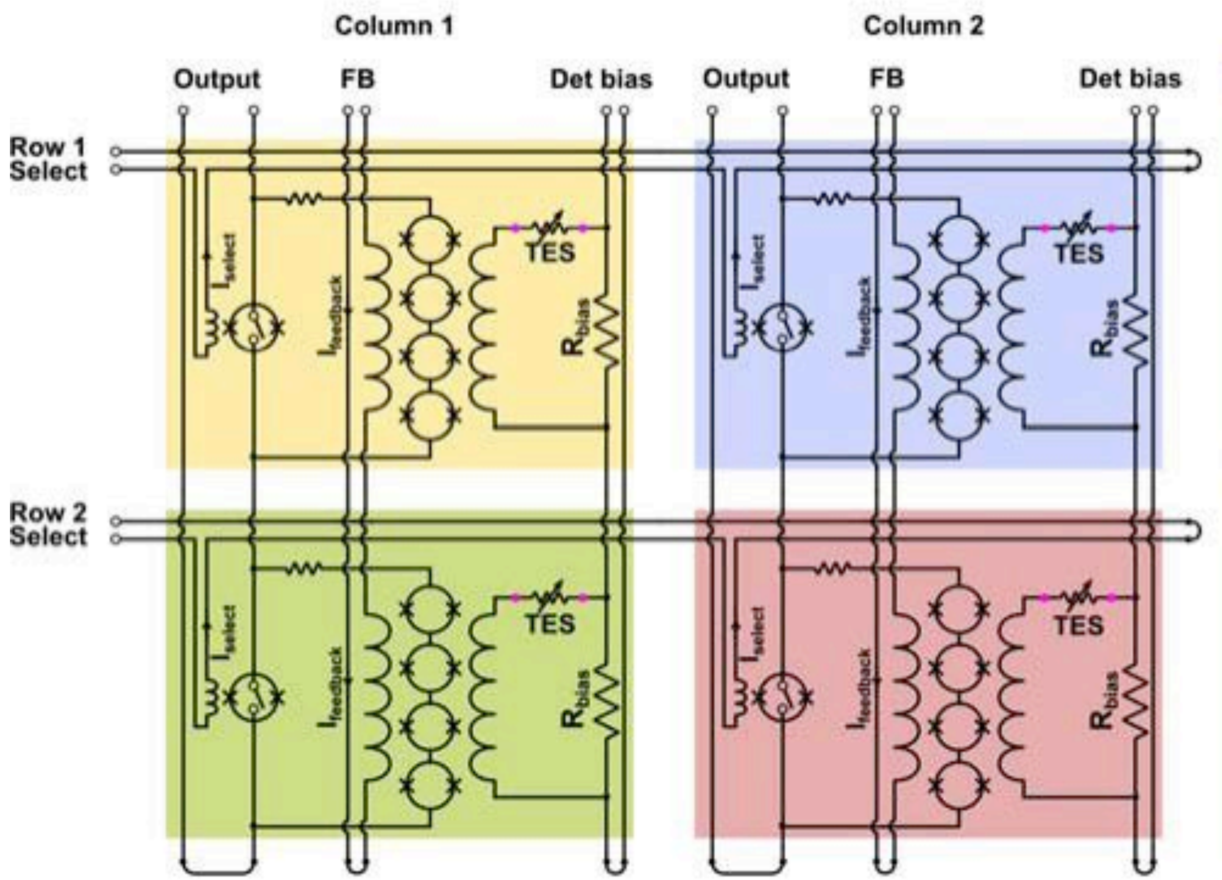

- 40 rows total

Flux-Switched Time-Domain Multiplexer

- Row Select switches current into switch inductor
- Switch critical current is large when flux is zero, hence is in superconducting state and shorts out SQUIDs → channel off
- Switch critical current near zero at some applied flux ($\Phi_0/2$) and acts like a resistor (ohms), biasing SQUIDs → channel on
- Switching set by geometry of inductance

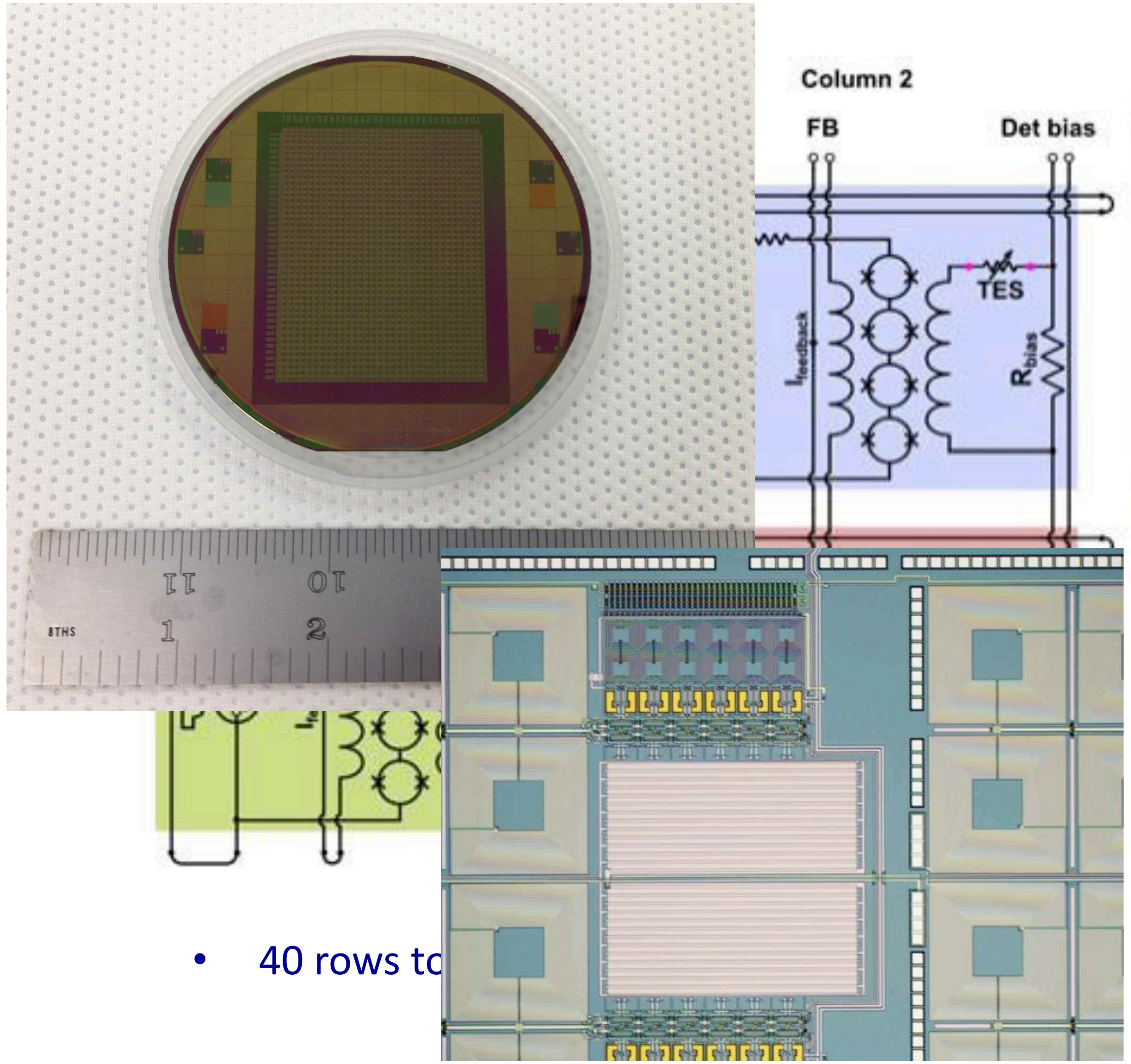

- 40 rows to

Through-Wafer Via

- TES routed to SQUID by Through-Waver Via

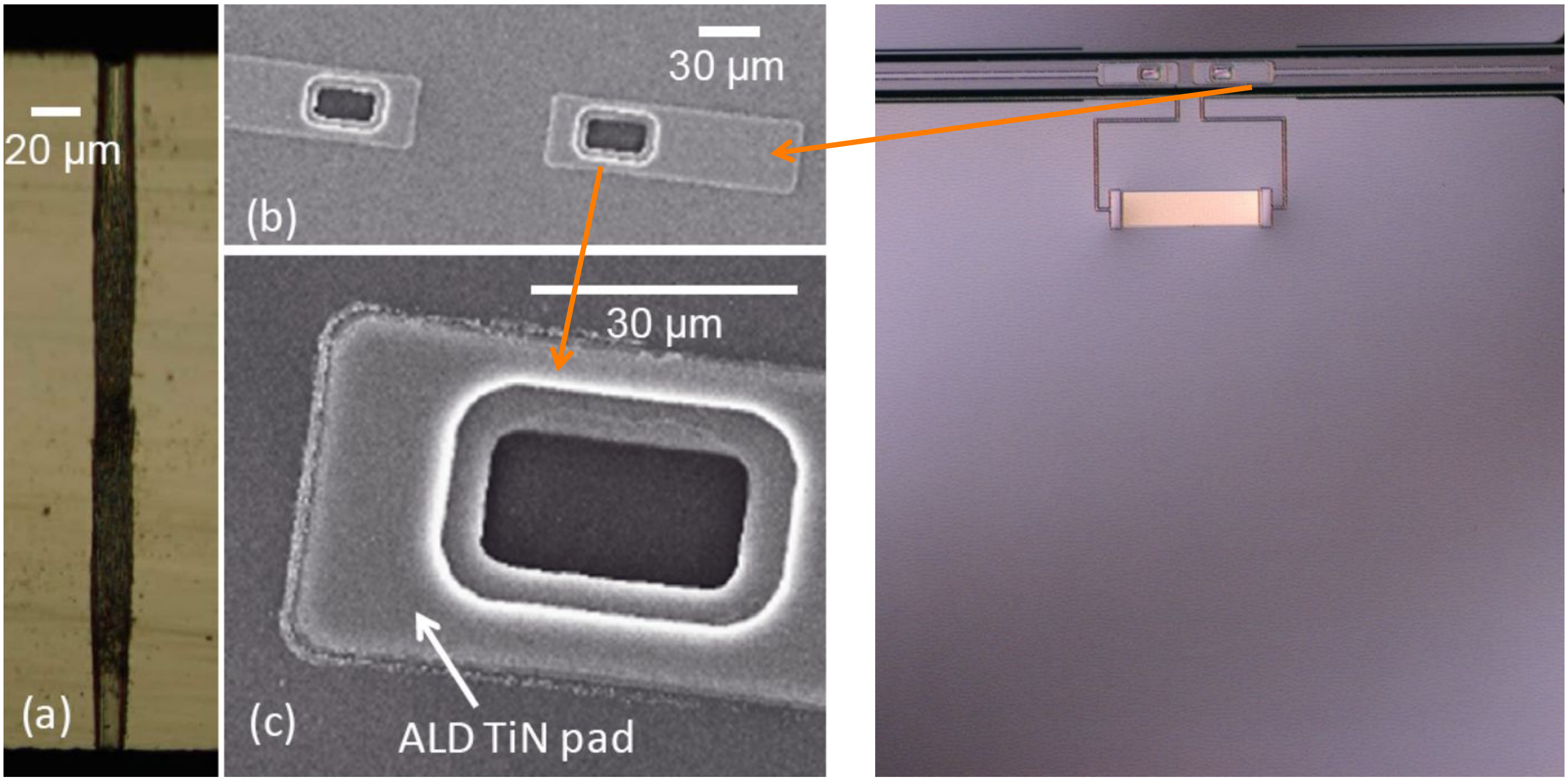

Array Hybridization: Bump Bonding

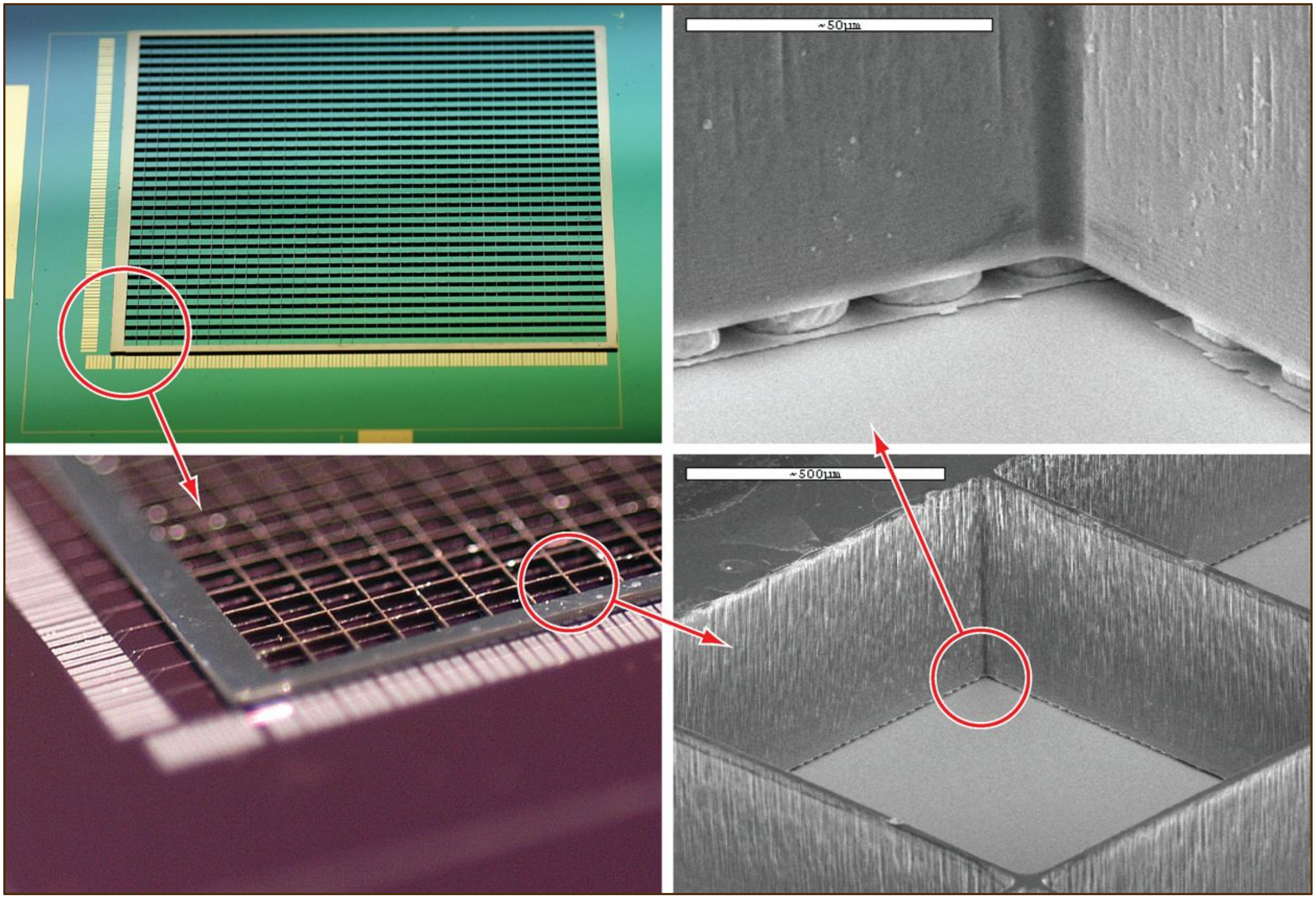

HAWC+ Detector Packaging

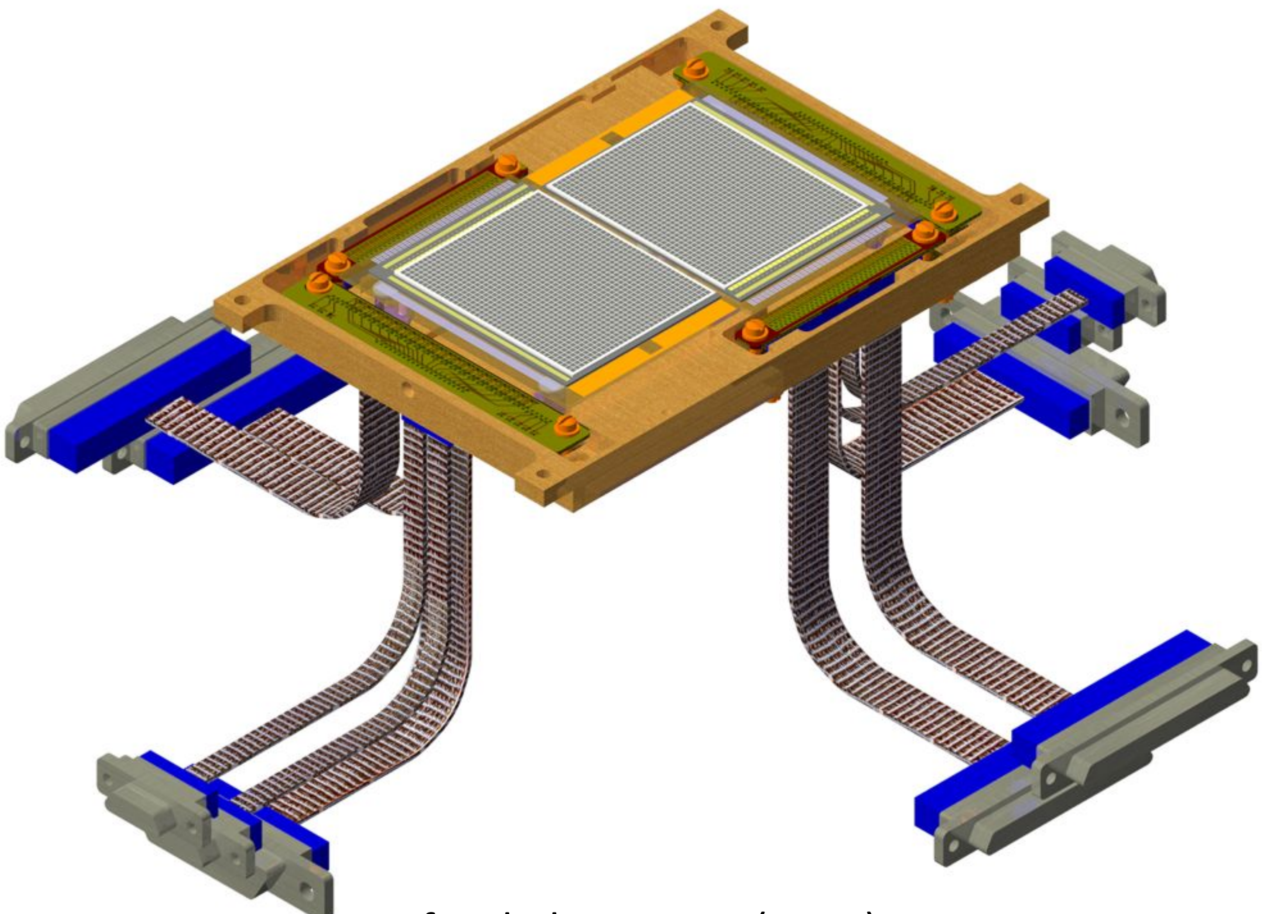

focal plane array (0.1 K)

HAWC+ Detector Packaging

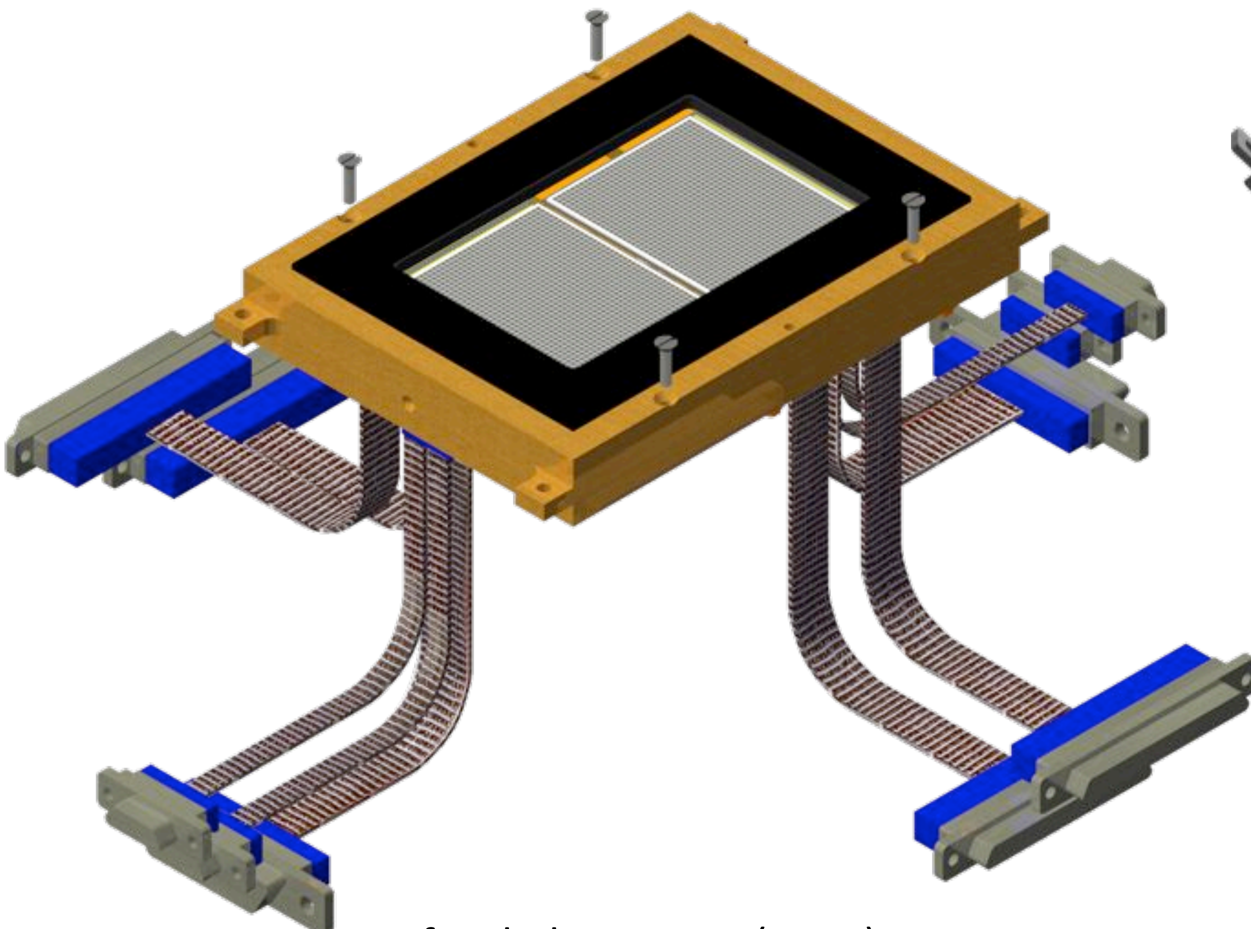

focal plane array (0.1 K)

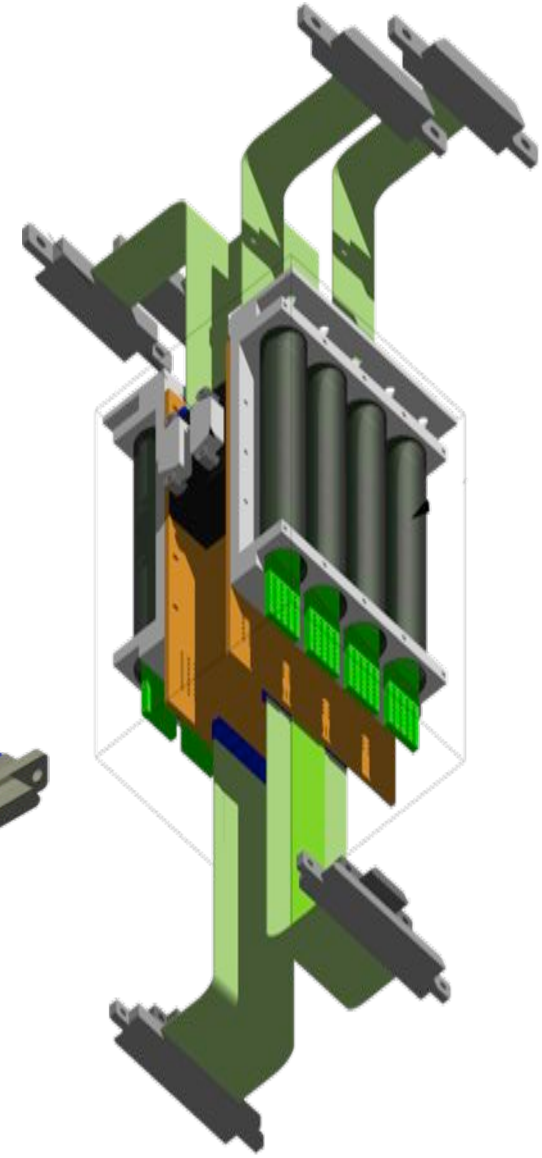

SQUID Series Array amplifiers (4 K)

room-temp. readout electronics: MCEs

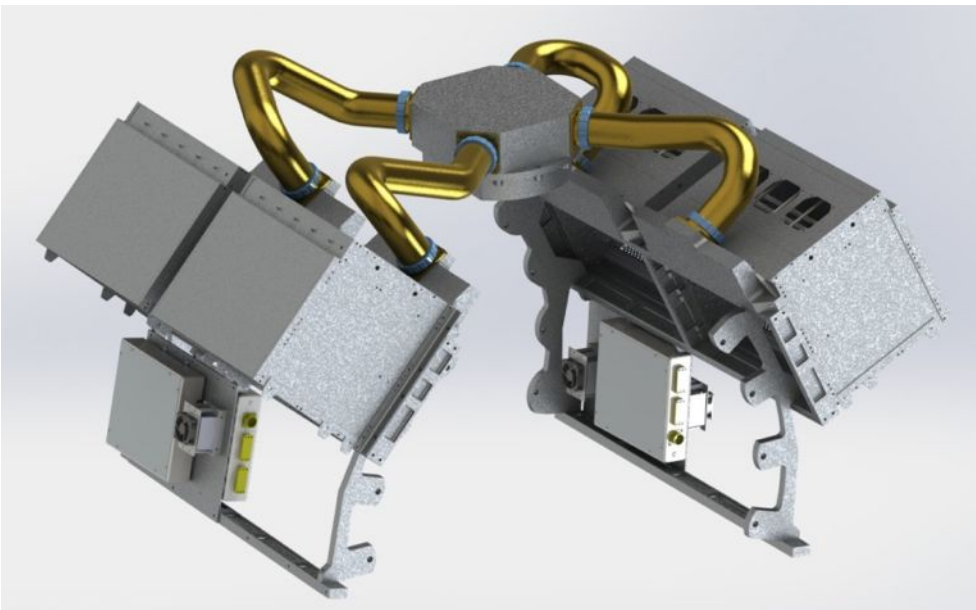

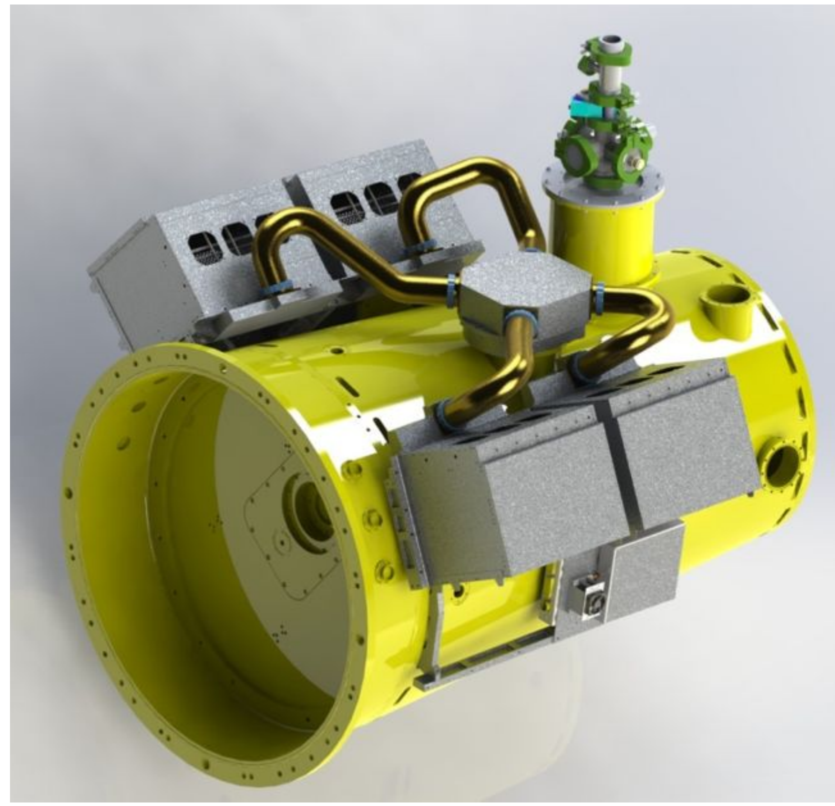

MCE readout system on HAWC

- SQUIDs are operated, and TESs biased, with Multi-Channel Electronics from U. British Columbia (originally designed for SCUBA2)
- 4 crates, each supporting 32x40 detectors
- Also shown: wiring feedthrough and conduit, DC-DC converters

detector specifications

Performance Parameter	Design Value	Comments
array format	32x40 elements, 1.135 mm pitch	2 arrays, each with design supporting 64x40
quantum efficiency	50%	for 1 mm^2 area
TES transition temperature	300 mK	
operating temperature	130 mK	
thermal conductance	1.5 pW/mK	at transition temperature
saturation power	140 pW	>300K load in all bands
electrical NEP	7.5×10^{-17} W $Hz^{-1/2}$	referred to absorbed power; photon: ≥ 2×10^{-16} W $Hz^{-1/2}$
time constant (natural)	1.7 ms	C/G
time constant (effective)	~200 μs	with feedback

HAWC+ Thermal Block Diagram

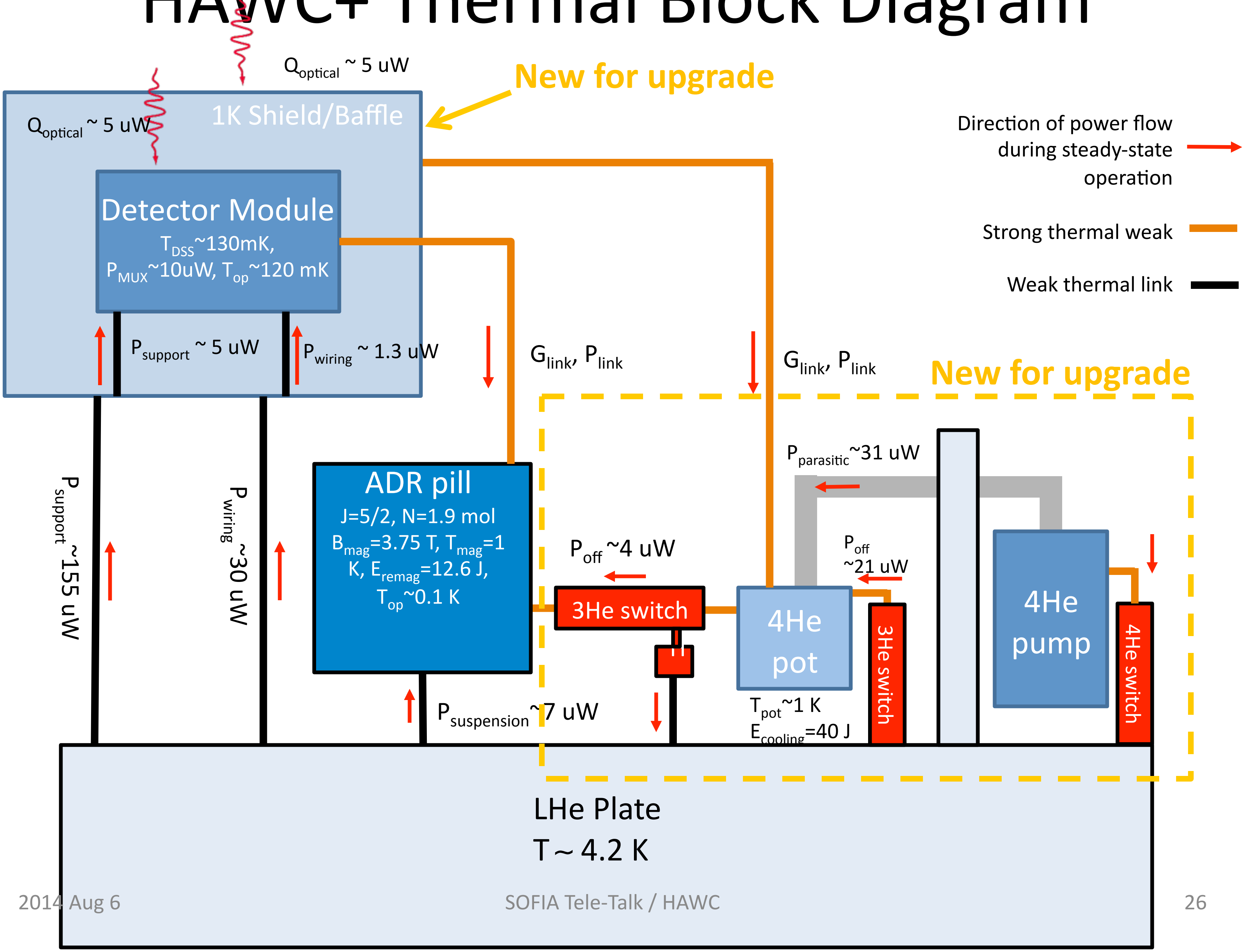

HAWC+ Thermal Block Diagram

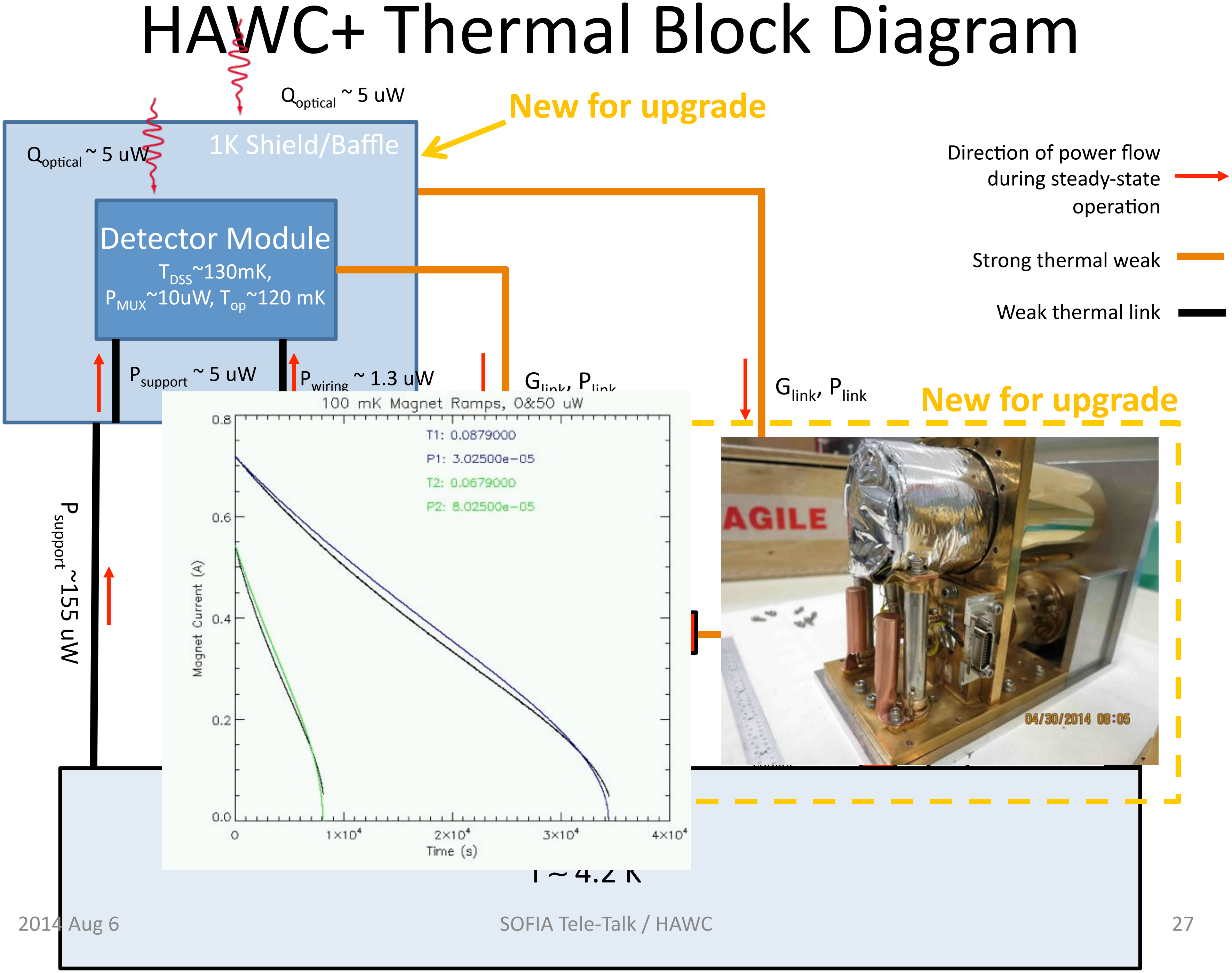

Cross-Section of Focal Plane Assembly

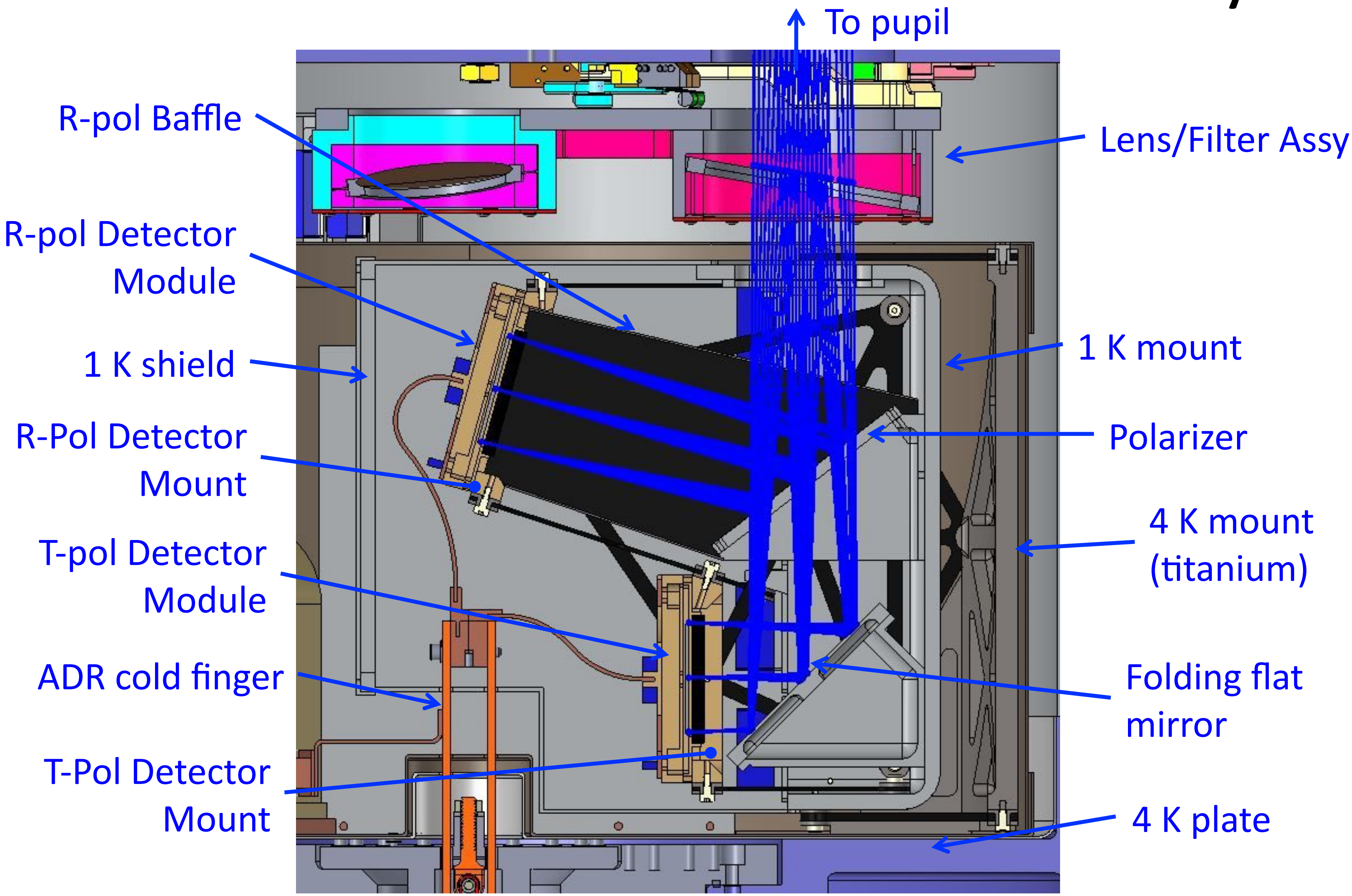

Cold Plate Arrangement

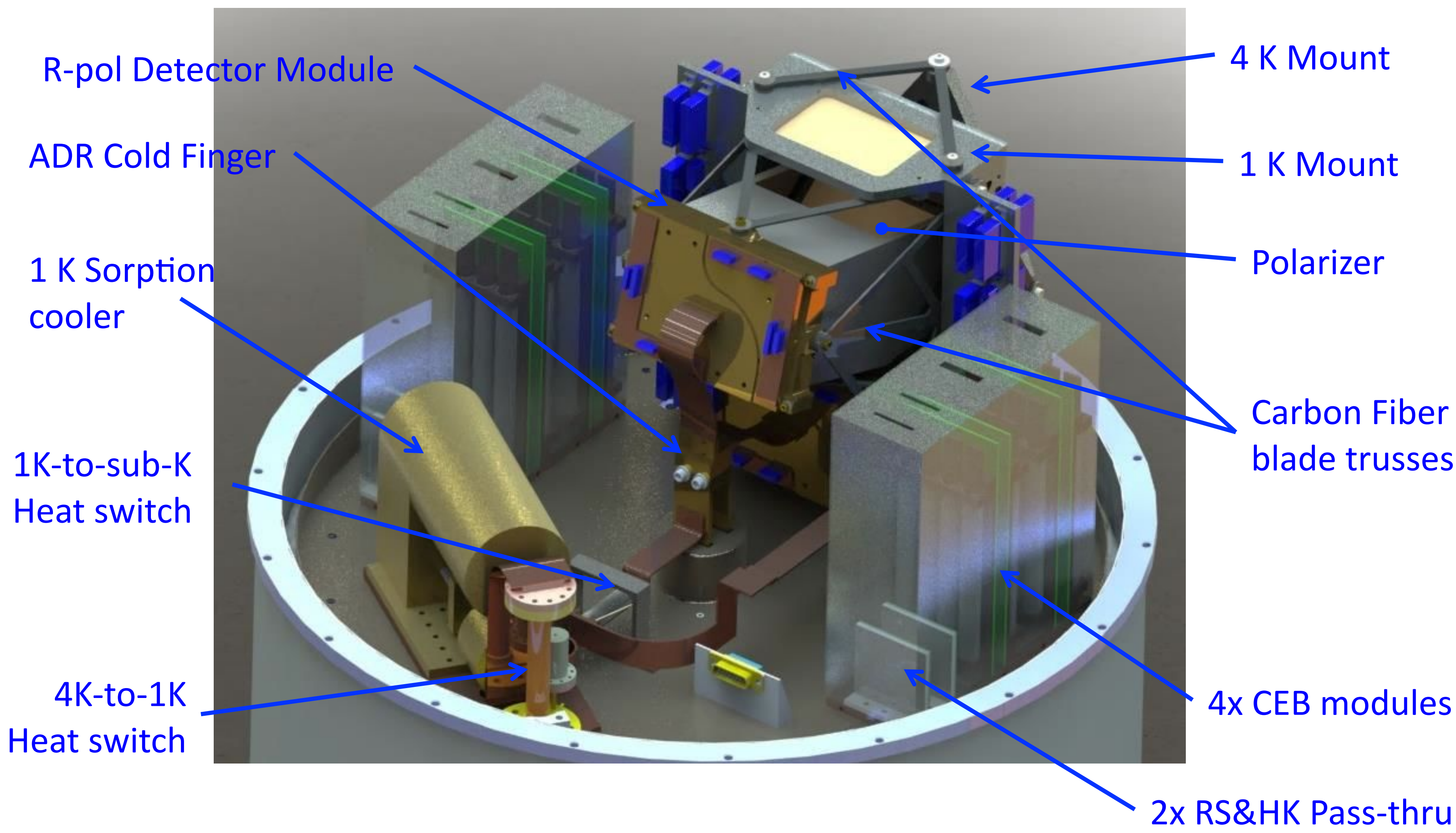

Magnetic Shielding

- Mag shielding plan employs multiple layers of superconducting and high-mu materials.

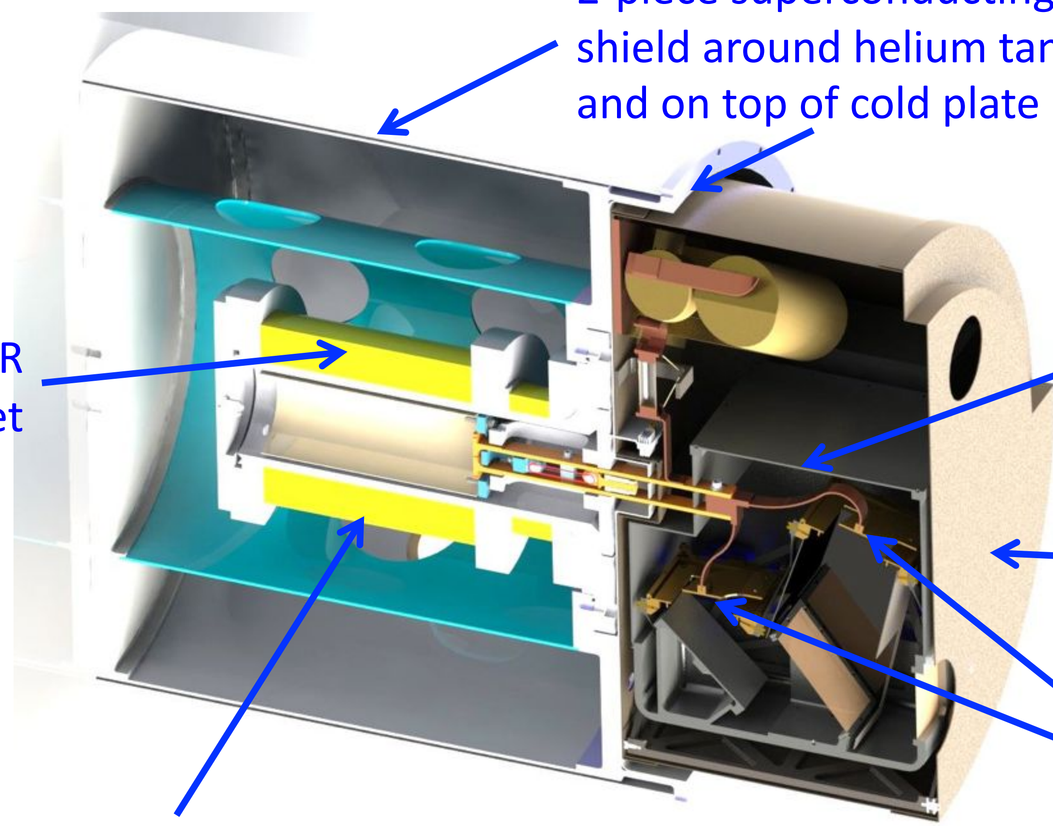

Mag Shield Model Performance

Max field strength at initiation of temperature control (0.5 T field at magnet bore): ignoring Earth's field.

Have to model each cutout in SC shield separately.

Light entrance to SC shield

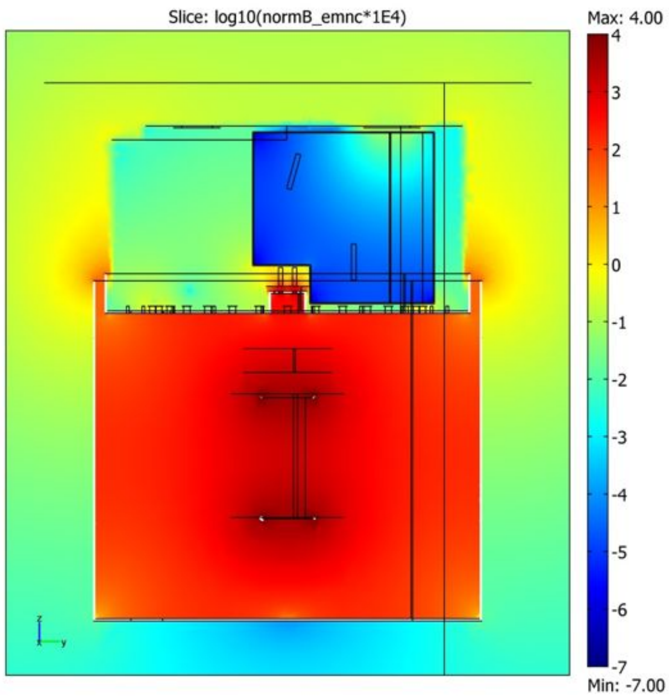

ADR penetration to SC shield

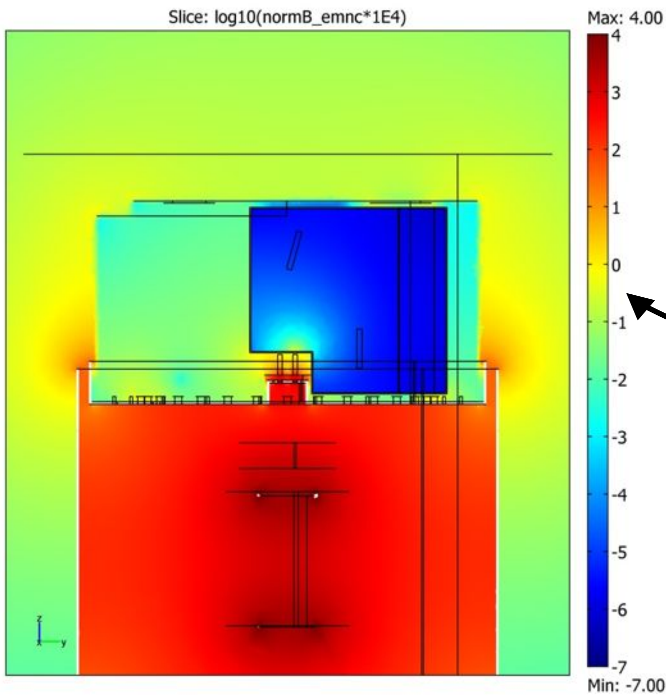

Field strength at DSS SQUIDs from ADR at initiation of temperature control is well below 0.345 G requirement.

HAWC Optics

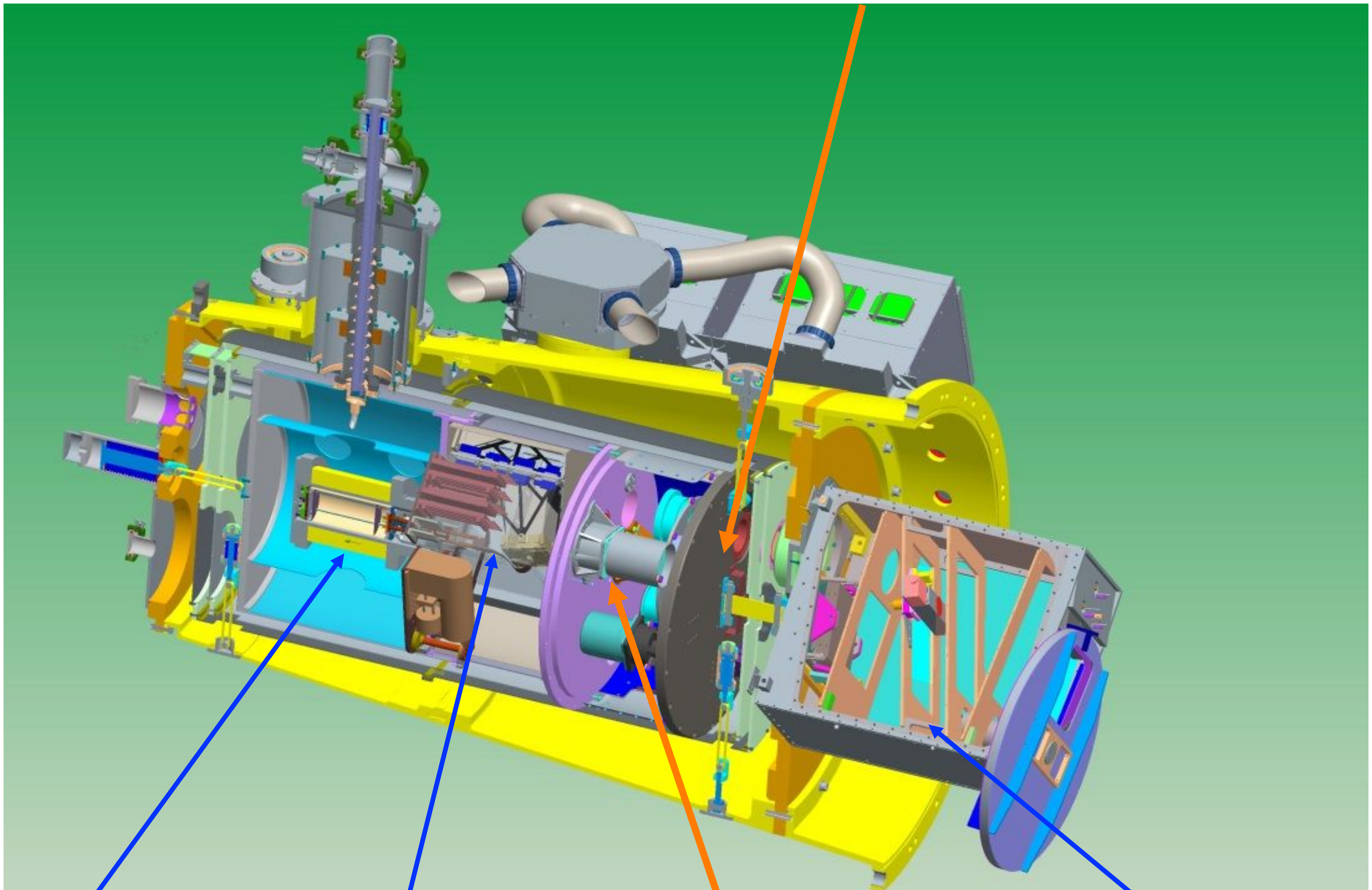
Pupil Assembly/Polarimeter
LHe / ADR
Detectors
Filter/Lens Assembly
Foreoptics

Polarimeter Mechanisms

- Carousel rotates to select one of four half-wave plates, imaging aperture, or one of three offset apertures.
- Each rotating half-wave plate is suspended with a grooved disc and three Vespel wheels. Each of the wheels is held with ball bearings on its axis, and one wheel is mounted with a flexure which displaces in the plane of the wheels.
- The half-wave plate disc is magnetically coupled to a drive disc, which is edge driven by the "mouse" motor, through a gear coupling.

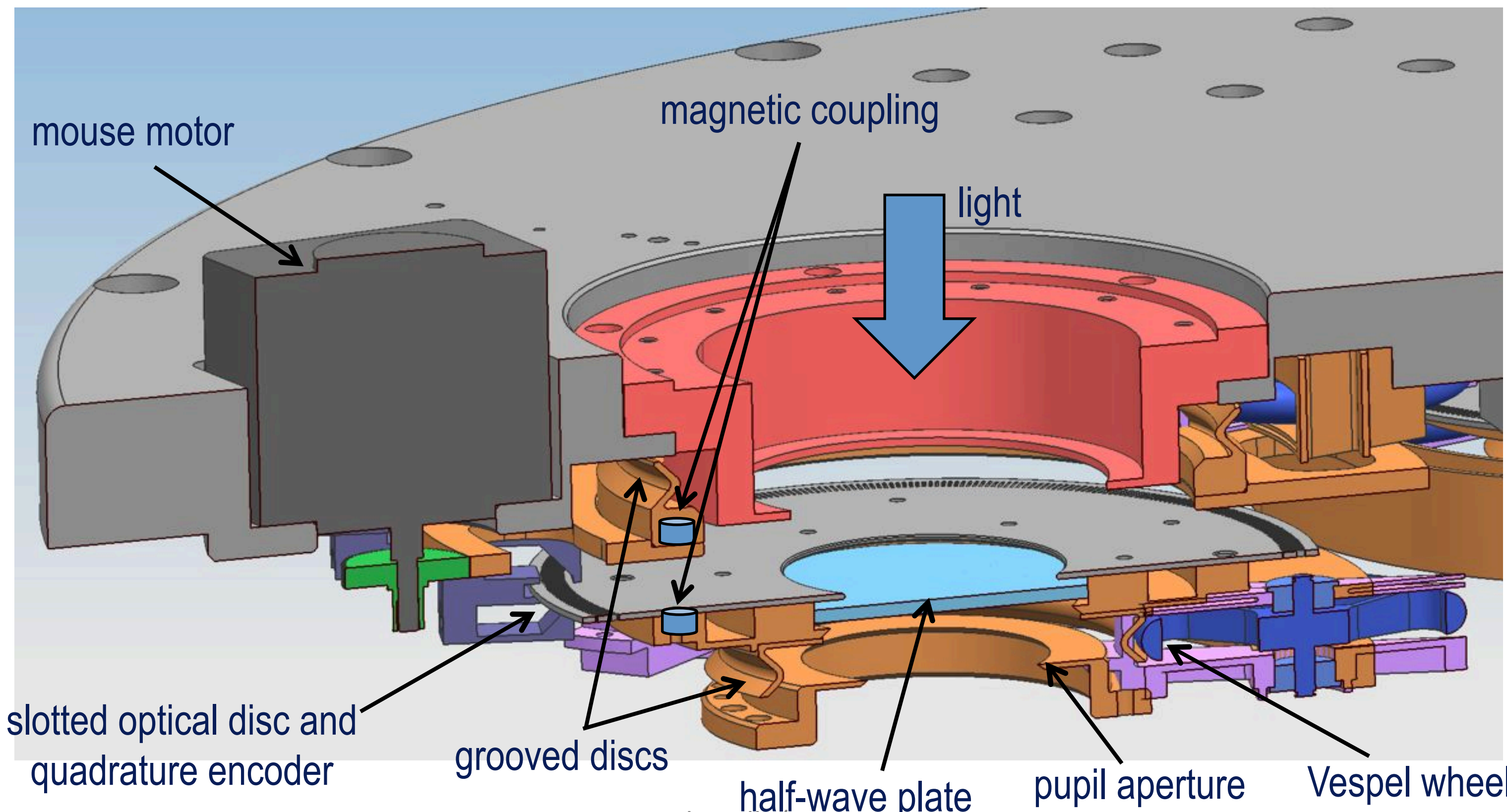

HAWC & Polarimeter Testing (July 2014)

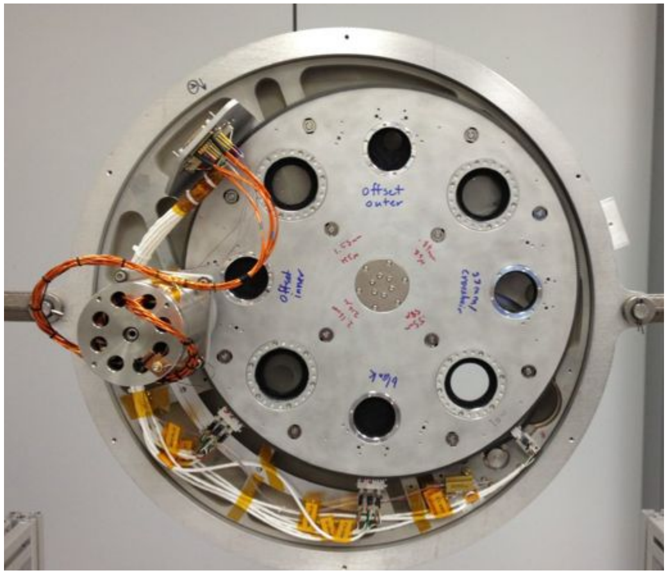

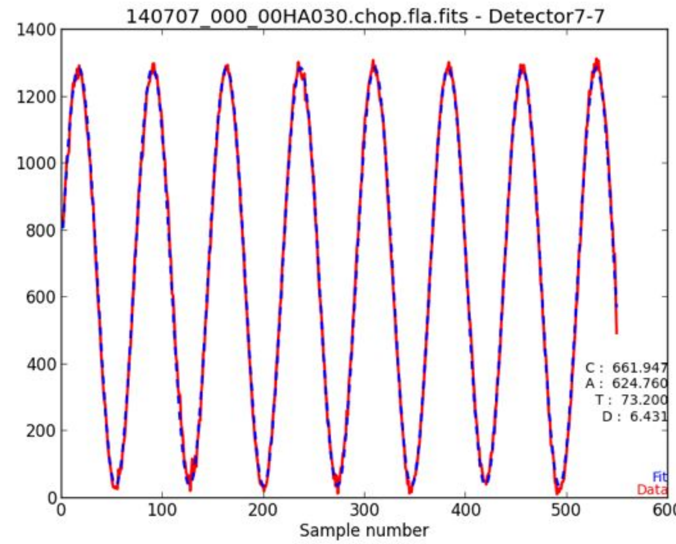

- Shown is the signal for one detector as half-wave plate is rotated, observing a highly polarized source, in 62 μm band.
- >85% polarization modulation efficiency in each of the 5 bands.

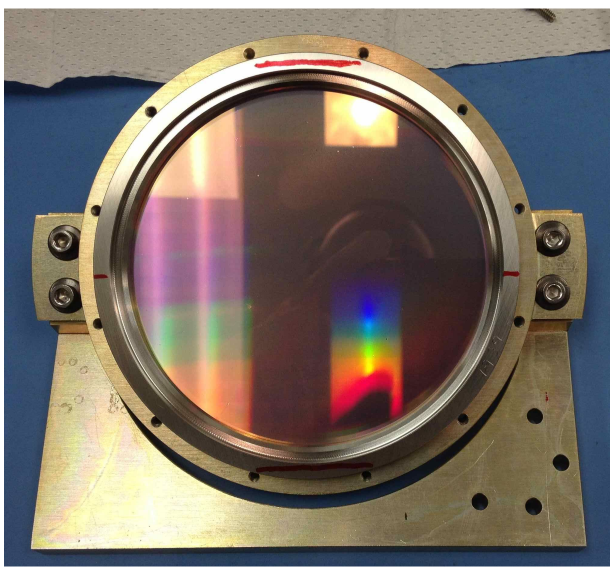

- Instrumental (false) polarization is on average low, < 0.5%, in each band.

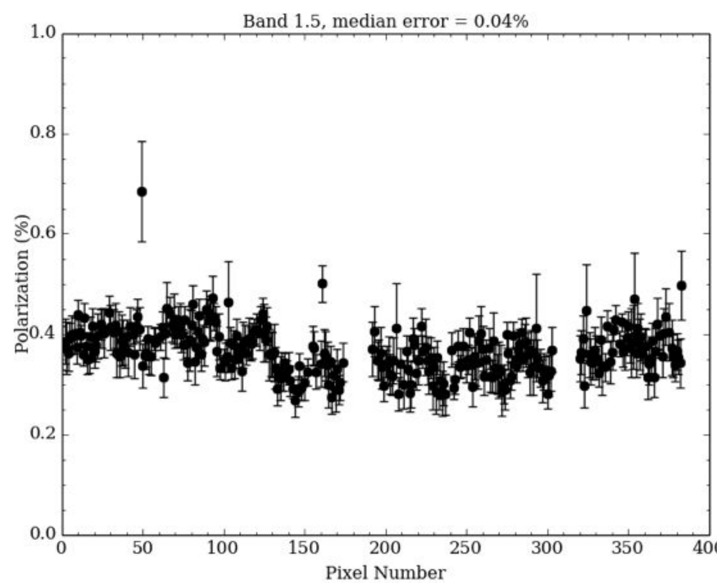

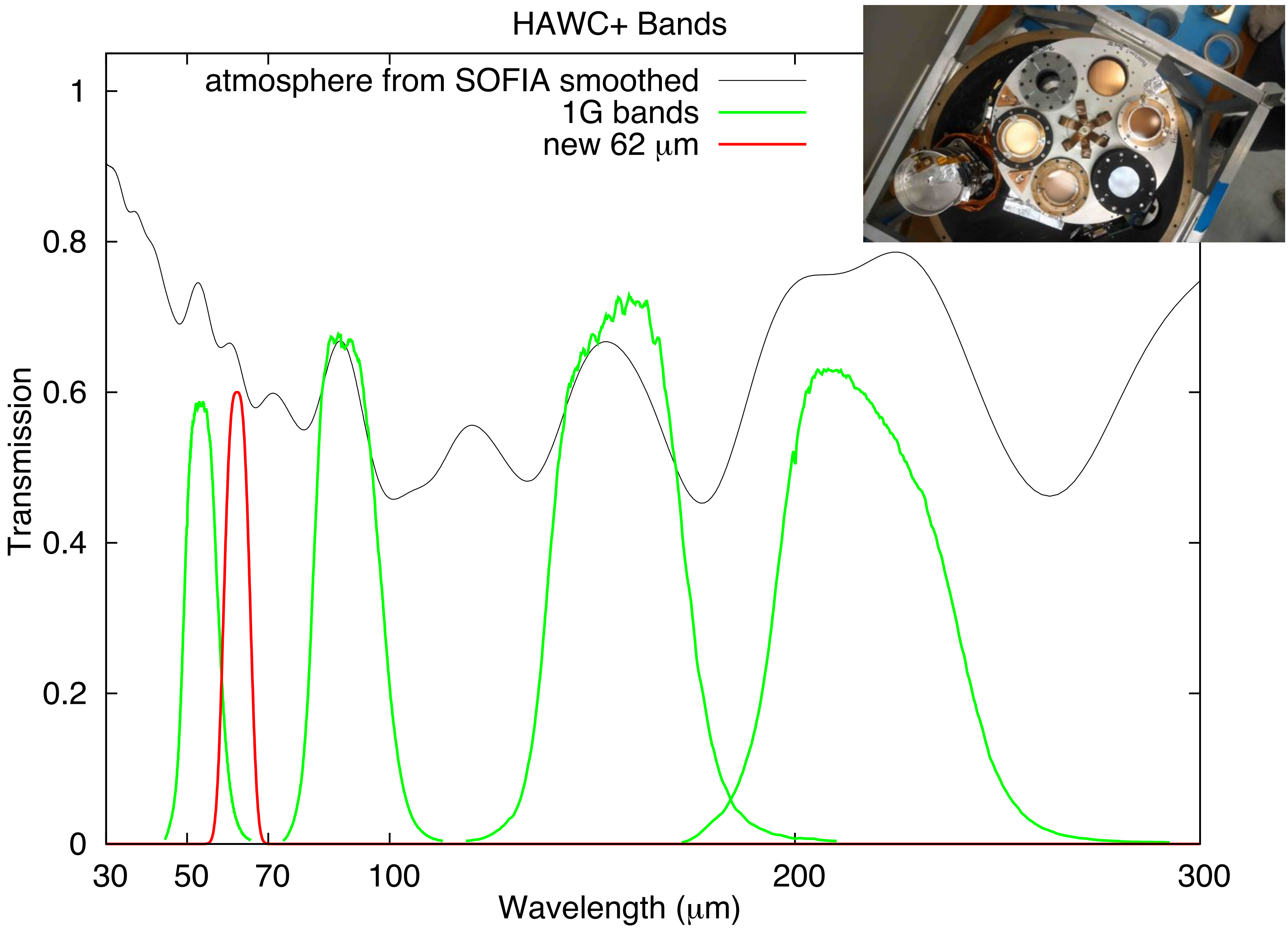
HAWC+ Bands
atmosphere from SOFIA smoothed
1G bands
new 62 μm
Transmission
0
0.2
0.4
0.6
0.8
1
30
50
70
100
200
300
Wavelength (μm)

HAWC Observing Modes

- polarimetry:
  - Traditional chopping and nodding
  - combined with stepped rotation of half-wave plate (possibly slow rotation in future)
  - Gives (I,Q,U) Stokes parameters
- imaging only:
  - Preference is to use a cross-linked scan (without chopping) for best sensitivity and fidelity.
  - Used efficiently on CSO and elsewhere.

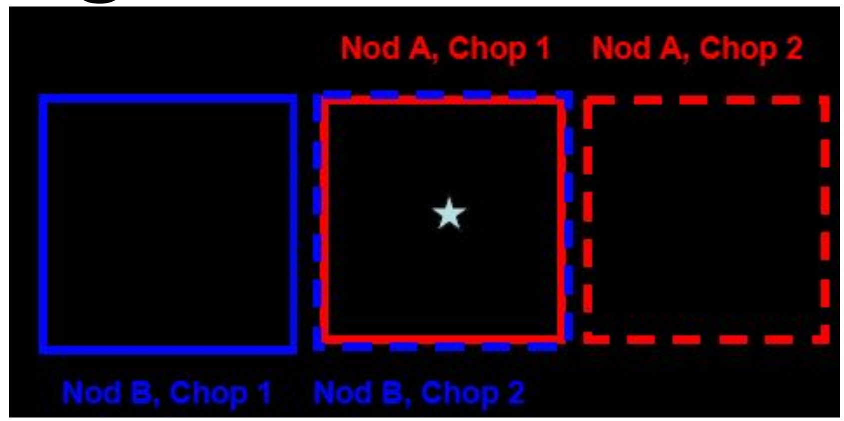

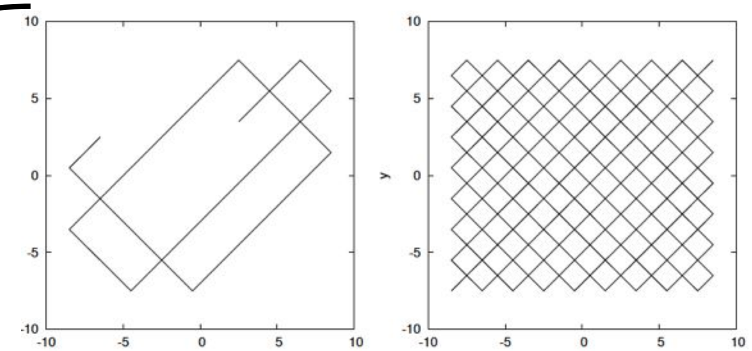

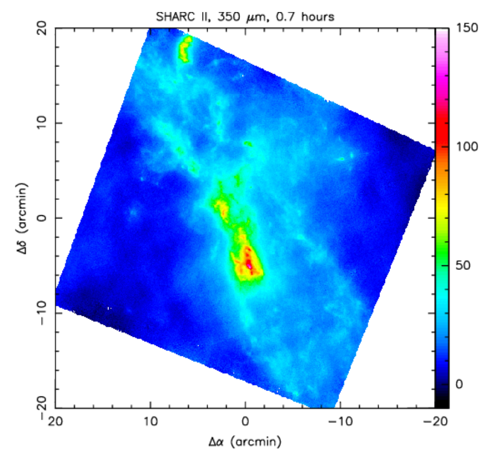

HAWC Data Acquisition Software

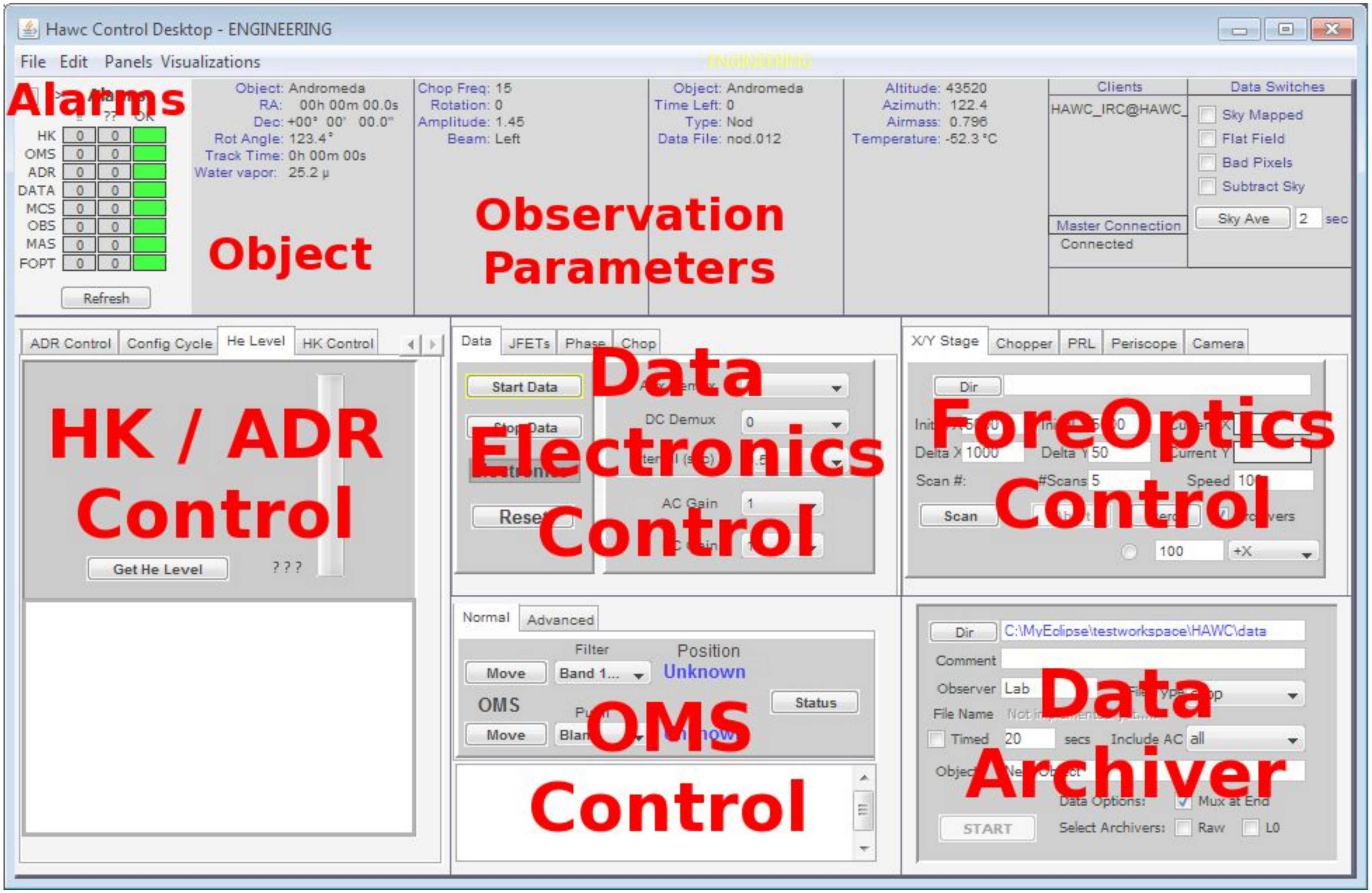

- We are adding new upgrade features into HAWC(1G) Java-based Control and Data Handling software (related to IRC).

HAWC Data Acquisition Software

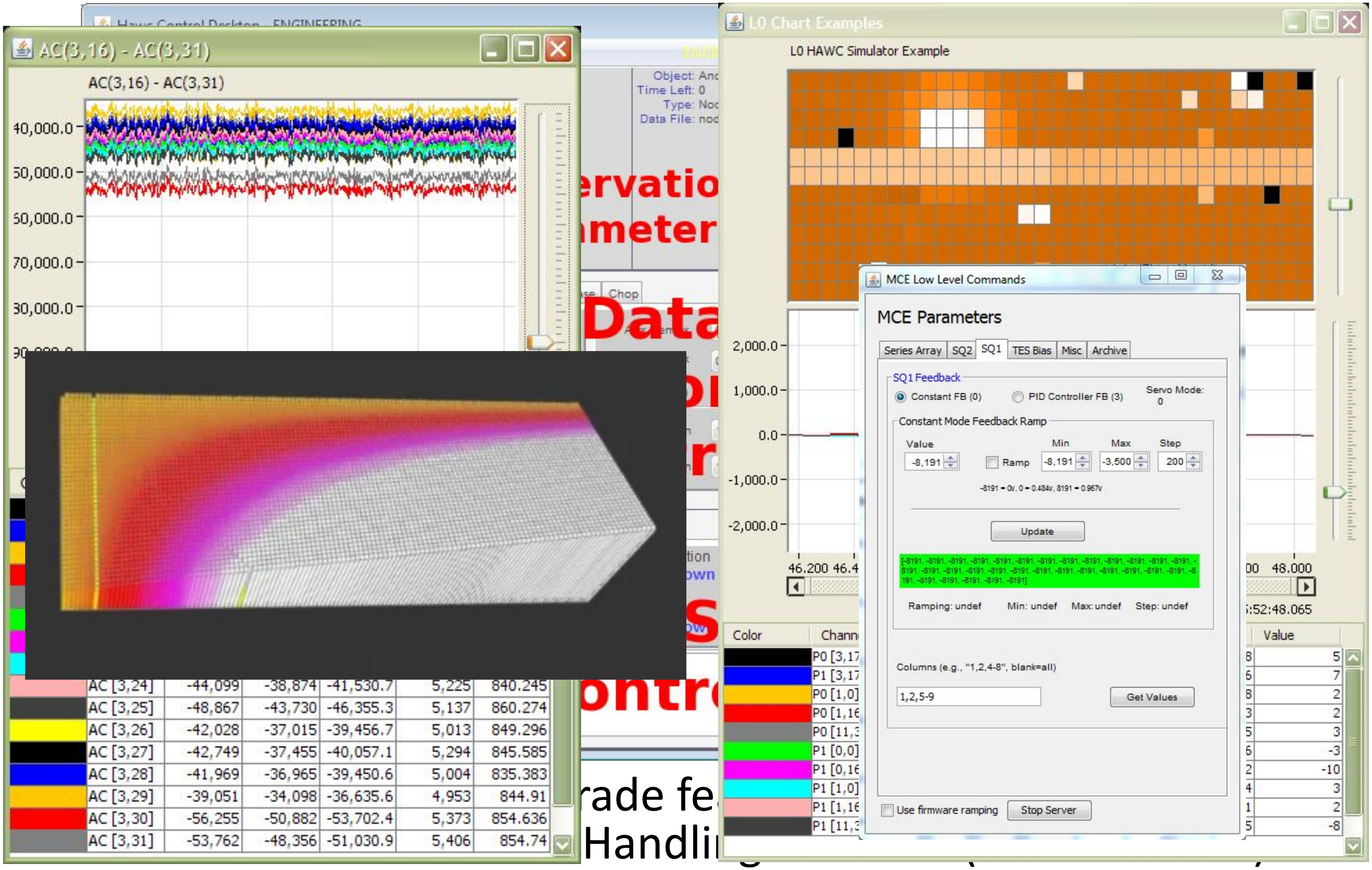

Polarimetry, Level 0 to 1.5

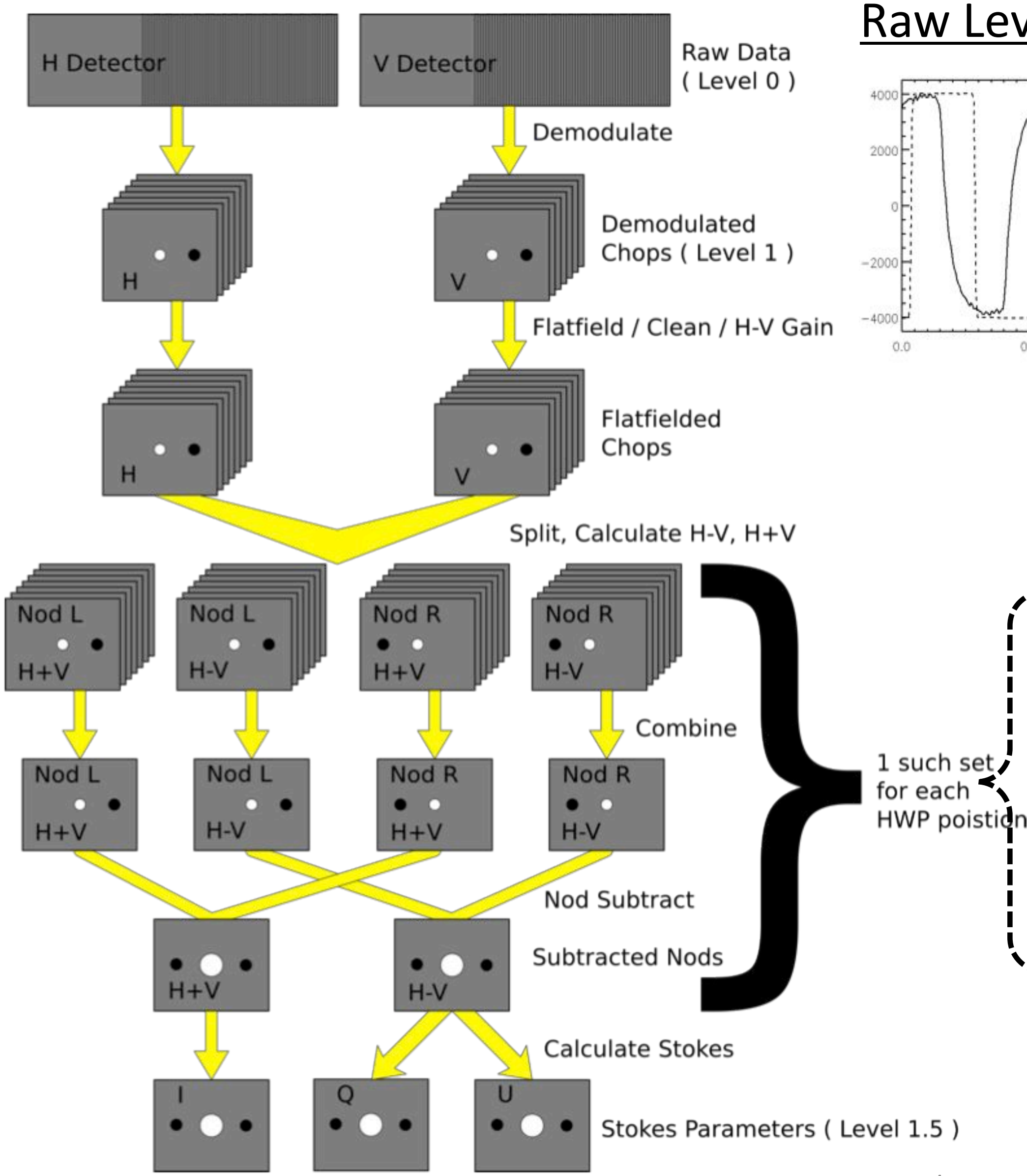

Raw Level 0 data, 100-1000 Hz sample rate

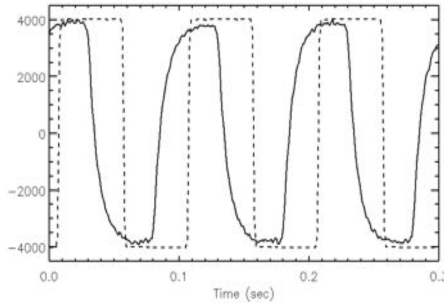

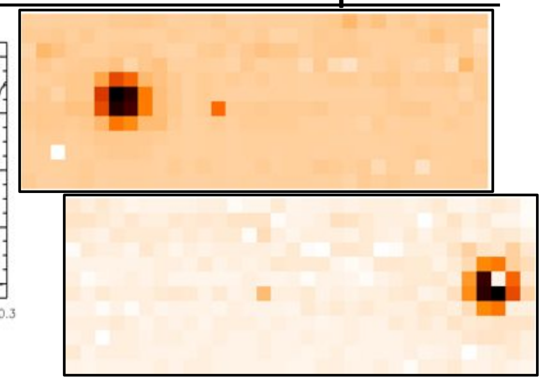

Data cube: $N_x \times N_y \times N_{\text{chop}} \times 2$

Split Nods:

$$N_x \times N_y \times \left[\frac{N_{chop}}{N_{nod}}\right] \times N_{nods} \times 4$$

Average chops in nods:

$$N_x \times N_y \times N_{\text{nods}} \times 4$$

Subtract nods & Average:

$$N_x \times N_y \times N_{\text{stokes}}$$

HAWC Predicted Performance

HAWC+ predicted performance for continuum imaging and polarimetry.

Instrument	Instrument Parameter	Band A	Band B	Band C	Band D	Band E
HAWC and HAWC+	wavelength (μm)	53	62	89	155	216
	angular resolution (arcsec FWHM)	5.4	6.4	9.0	16	22
	imaging NEFD[a] (Jy/beam $s^{1/2}$)	0.93	0.80	0.79	0.64	0.55
HAWC+	field of view (square arcmin)	4.6	11	11	33	59
	min. flux density[b] for s(P) < 0.3% in 1 hr (Jy/beam)	10.7	9.2	9.1	7.3	6.3
	min. surface brightness[b] in 1 beam for s (P) < 0.3% in 1 hr (MJy/sr)	13,500	8200	4100	1090	480

[a]Noise Equivalent Flux Density gives the flux density detectable with signal-to-noise=1 in a 1 second integration time. Signal-to-noise scales as (flux/NEFD) × $(\text{time})^{1/2}$.

[b]Assumes 60% observing efficiency and an instrument such as HAWC+ which simultaneously detects two polarization states. The quantity σ(P) refers to the uncertainty in the measured degree of polarization, expressed as a percentage.

HAWC Project Dates

- 2014 January 10-11: Critical Design Review
- 2014 May-July: polarimetry with 12x32 array
- 2015 March: new detector arrays integrated into HAWC; final system test runs
- 2015 August: HAWC delivered to Palmdale AOF
- 2015 October: first commissioning campaign on SOFIA
- 2015 December: second commissioning campaign; first science campaign

HAWC/SOFIA Science Goals

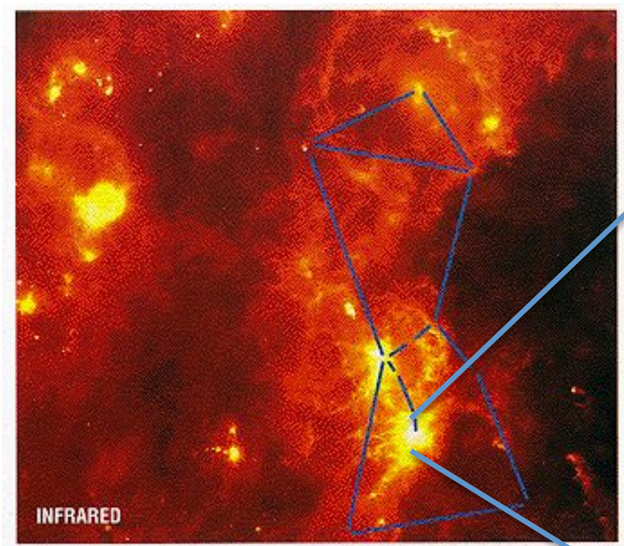

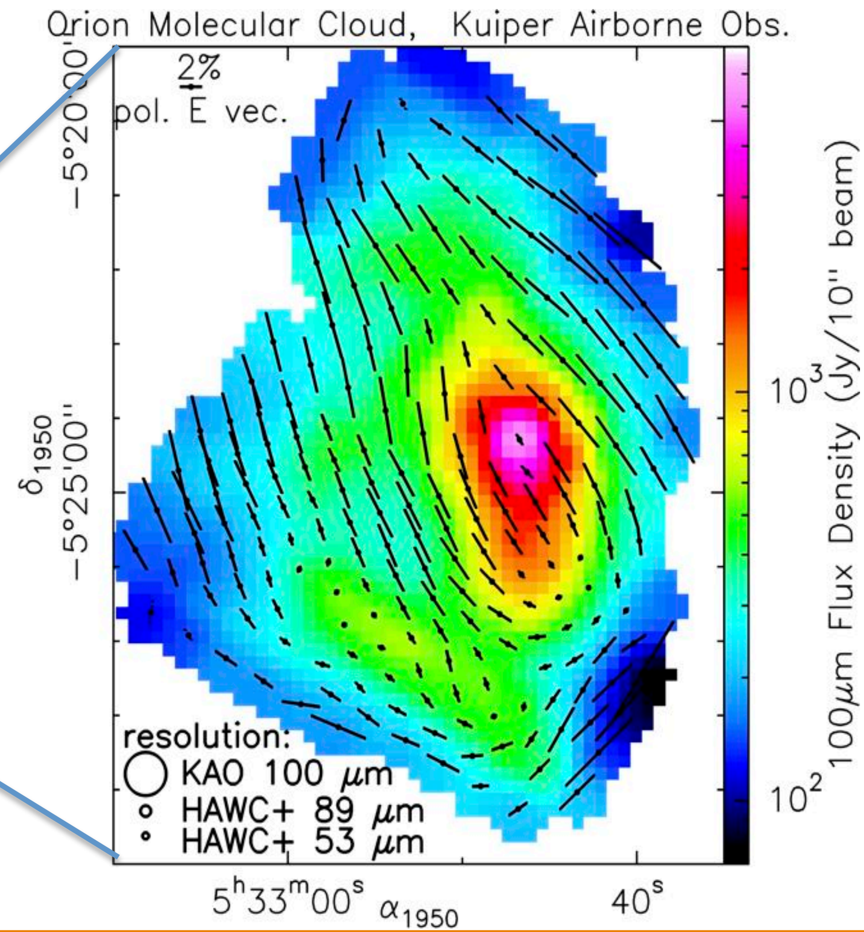

- Compared to previous facilities (e.g., KAO polarimetry):
  - 8× more sensitive to extended emission (can reach $A_V \approx 1$)
  - 50× more sensitive to point sources
  - 10× better areal resolution
  - 20× as many imaging elements
  - 5 wavelength bands instead of 1

- tests of (ordered) magnetic field models
- statistical estimation of field strength (Chadrasekhar-Fermi, structure function)
- tests of grain alignment theory (Radiative Aligning Torques)

Galactic Center

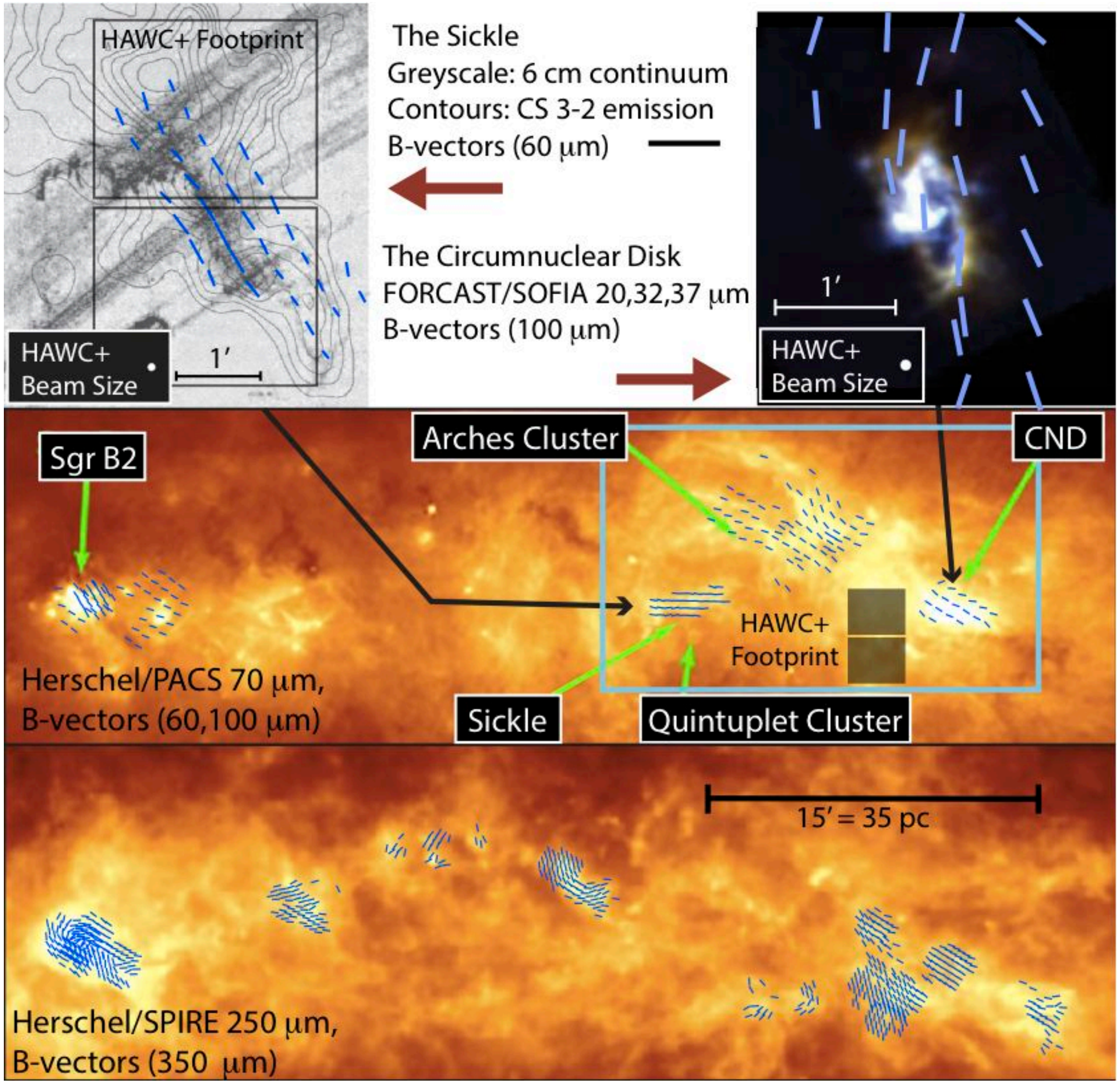

The blue region can be mapped in part of a single SOFIA flight, resulting in ~10,000 detections of polarization.

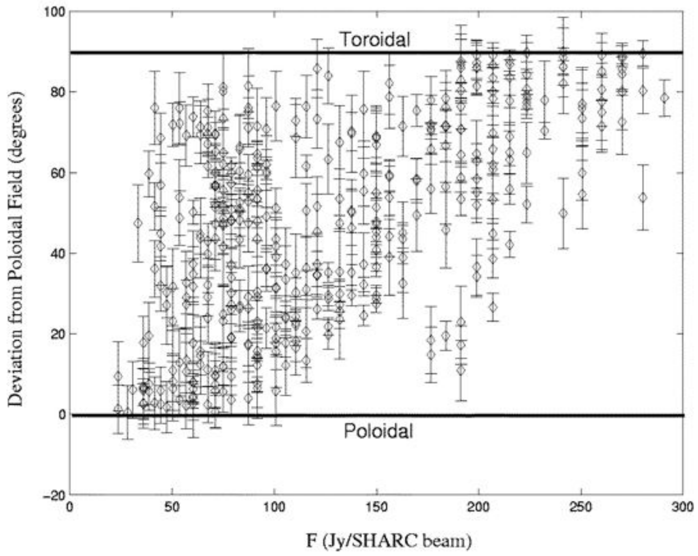

Chuss et al. (2003): CSO and KAO polarization measurements suggest toroidal field in dense material and poloidal in more diffuse, consistent with model of Uchida et al. (1985).

Characterizing Magnetic Field Strength

Simulated Molecular Clouds

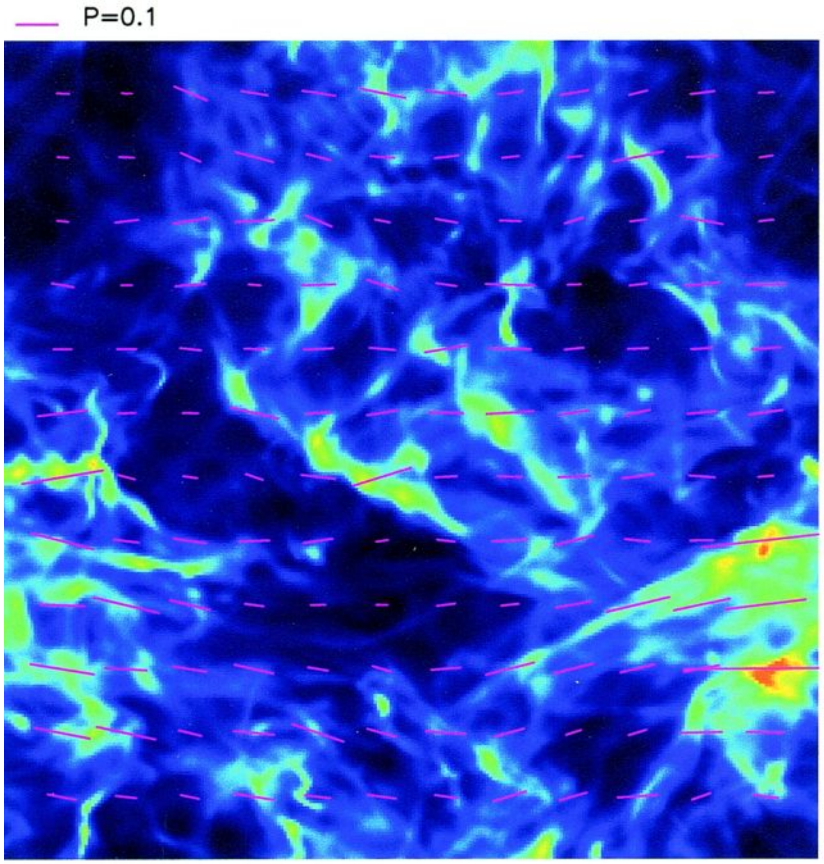

strong field – small dispersion

(Ostriker, Stone, & Gammie 2001)

- Approach based on Chandrasekhar & Fermi (1953)

$$\frac{B^2}{4\pi\rho\sigma^2(v)} \approx \frac{1}{(\Delta\phi)^2}$$

  - with modeling by several research groups to account for effects of beam and line-of-sight averaging
- Need velocity dispersion from submm/radio telescope observations of molecules.

Characterizing Magnetic Field Strength

Simulated Molecular Clouds

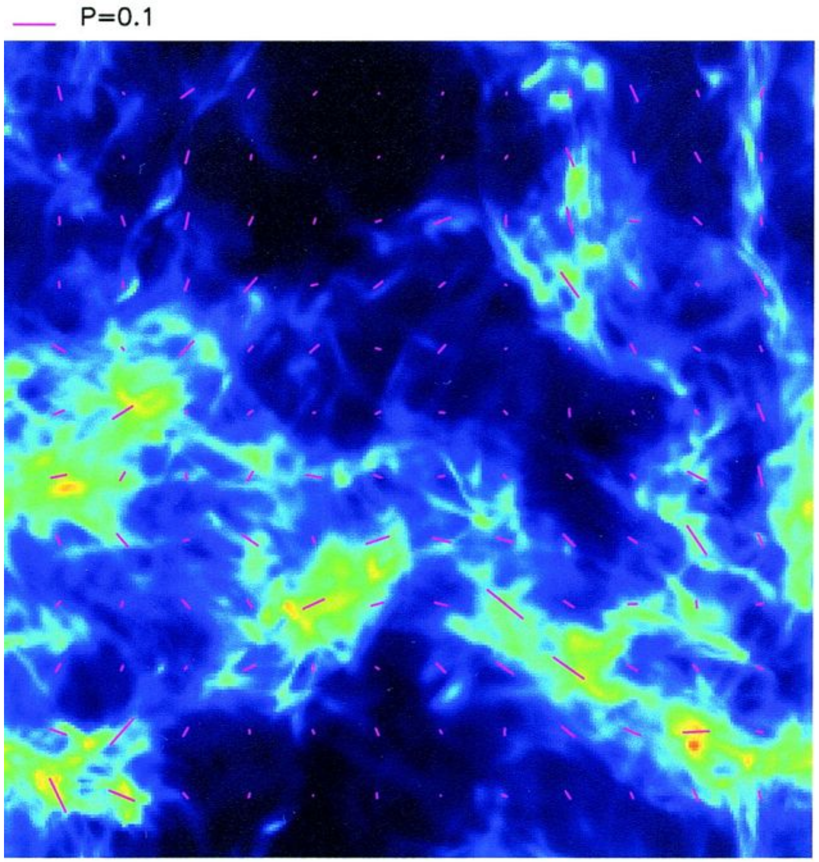

weak field – large dispersion

(Ostriker, Stone, & Gammie 2001)

- Approach based on Chandrasekhar & Fermi (1953)

$$\frac{B^2}{4\pi\rho\sigma^2(v)} \approx \frac{1}{(\Delta\phi)^2}$$

  - with modeling by several research groups to account for effects of beam and line-of-sight averaging
- Need velocity dispersion from submm/radio telescope observations of molecules.

Use of polarization angle structure functions to study power spectrum of magnetized turbulence

OMC-1

angle $\Phi(\mathbf{x})$

$$\Delta\Phi(\ell) \equiv \Phi(\mathbf{x}) - \Phi(\mathbf{x}+\ell)$$

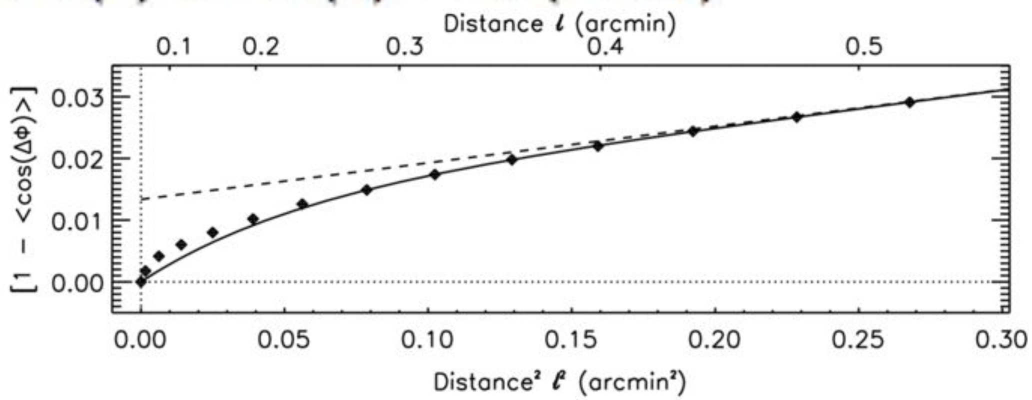

- magnetic field strength: ~0.8 mG

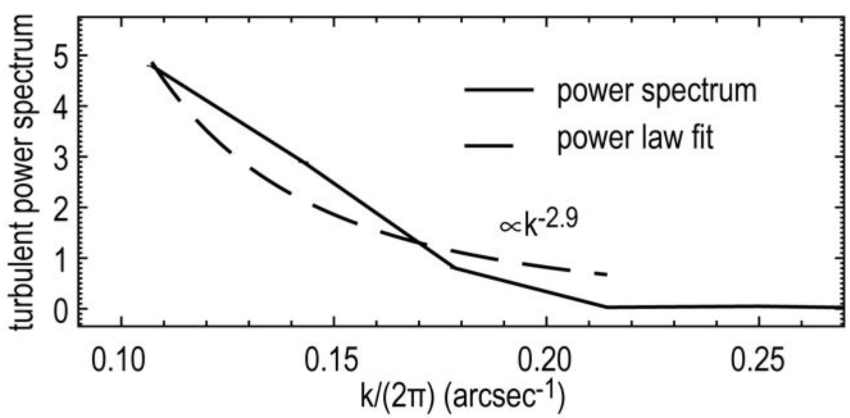

- dissipation scale: ~10 mpc

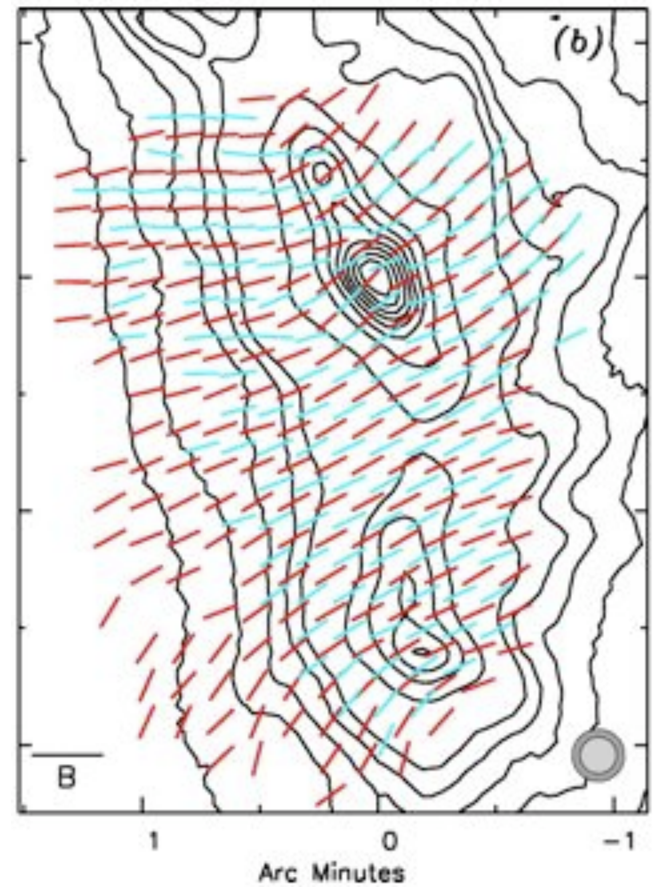

Hildebrand et al. '09; Houde et al. '09, '11

Dust Grain Alignment

- Dust grain alignment is an unsolved problem of astrophysics. Only recently has radiative alignment become favored theory over paramagnetic relaxation.
- No matter what, alignment is with respect to magnetic field: Larmor precession ($t \approx 10^6$ s) washes out alignment with respect to any other direction. (Martin 1971)
- Radiative alignment, requiring asymmetric grains and an asymmetric radiation field, is currently the leading theory (Dolginov & Mytrophanov 1976; Draine & Weingartner 1996/7; Lazarian & Hoang 2007).
  - Test #1: Does the degree of grain alignment depend on the strength of the radiation field?
  - Test #2: Is there spectral evidence for better alignment of large grains?

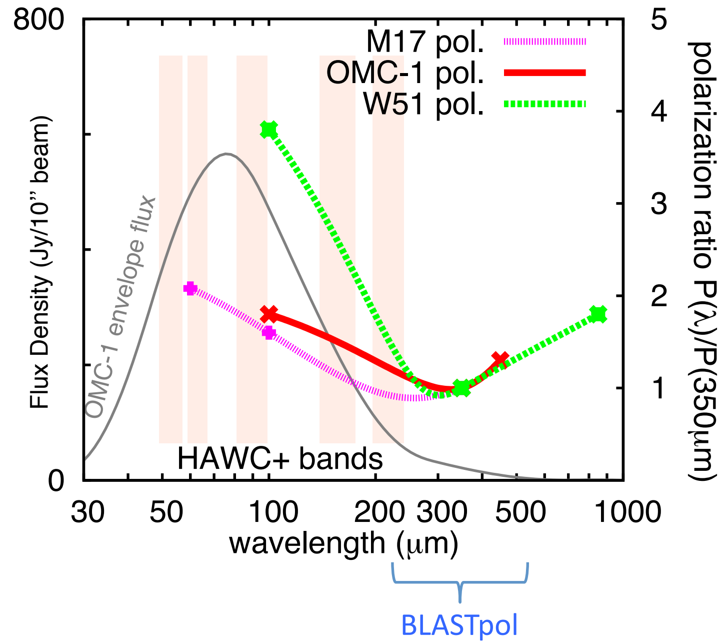

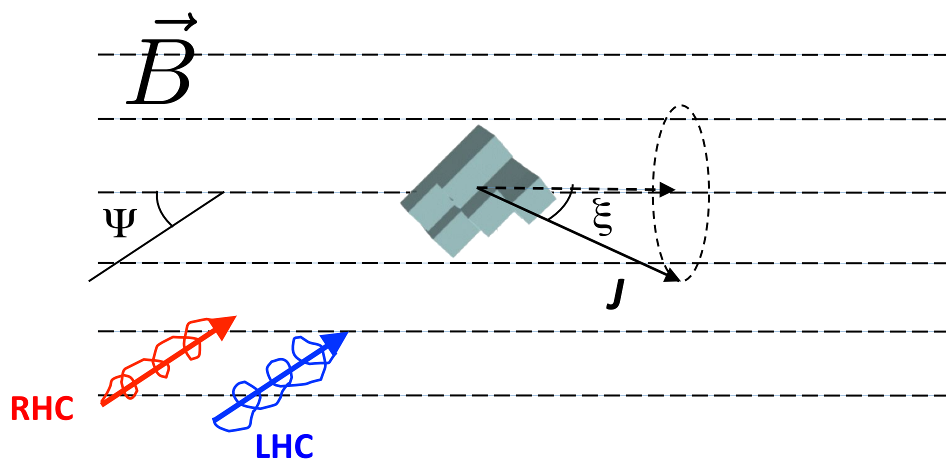

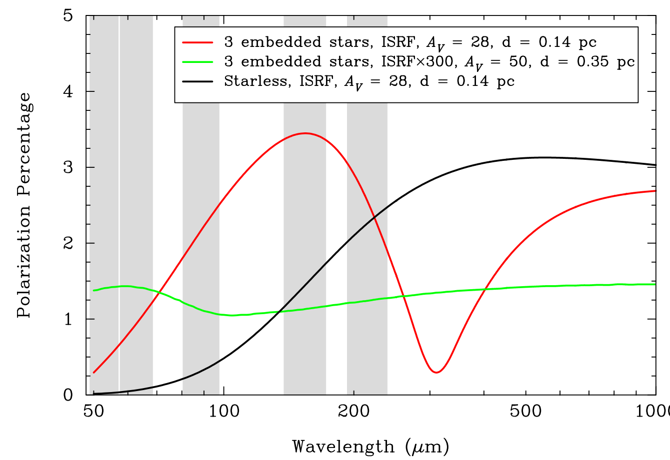

HAWC Project Dates

- 2015 March: new detector arrays integrated into HAWC; final system test runs
- 2015 Spring: SOFIA Cycle 4 proposal call
- 2015 August: HAWC delivered to Palmdale AOF
- 2015 October: first commissioning campaign on SOFIA
- 2015 December: second commissioning campaign; first science campaign